Department of Health Science and Technology
Aalborg university

AALBORG UNIVERSITET

THE CONSEQUENCES AND REVERSIBILITY OF CONGENITAL IRON DEFICIENCY ON THE AMOUNT OF NEURONS IN THE HIPPOCAMPAL AREA AND THE FATTY ACID COMPOSITION OF THE CEREBELLUM

Marco Gall

Master in Medicine with an Industrial Specialization
Aalborg university, 1st of June 2011
Supervisor: Professor Torben Moos

THE CONSEQUENCES AND REVERSIBILITY OF CONGENITAL IRON DEFICIENCY ON THE AMOUNT OF NEURONS IN THE HIPPOCAMPAL AREA AND THE FATTY ACID COMPOSITION OF THE CEREBELLUM

Marco Gall

Master in Medicine with an Industrial Specialization
Aalborg University 2011
Denmark

Abstract

Background: Iron deficiency is the most prevalent nutritional disorder worldwide, especially among pregnant women and children. Congenital iron deficiency causes several deleterious effects on the cognitive and motoric development of the infant.

Objective: The objective of this study is to assess the consequences of severe congenital iron deficiency on the neuron count in the hippocampus and the fatty acid composition of the cerebellum in male Wistar rats, and to discover whether or not iron supplementation injected during the window of opportunity, which is equivalent to the 3rd trimester in human development, can restore the deleterious effects of iron deficiency.

Design: Adult female rats were randomly divided into two groups. The rats assigned for iron deficiency were exsangiunated and fed an iron depleted diet (<10mg Fe/kg), while the control rats were fed a commercial diet. The offspring of the iron deficient (ID) dams were designated into two groups, a treatment group where pups received iron injections (45mg/kg iron isomaltoside 1000) and a group receiving saline injections, thus remaining ID. The severity of iron deficiency was confirmed by measuring hematocrit values on postnatal day (P) 8-13, P15-18 and P86-94. A footprint analysis test was performed on male rats on P85-90 and the rats were euthanized on P86-94, and their brains were excised for brain iron analysis of the mesencephalon, stereological analysis of the hippocampus and fatty acid analysis.

Results: The results of the footprint analysis showed significantly increased gait width in ID animals compared to both control and ID animals receiving iron supplement (ID + im1000). The fatty acid analysis showed a significant decrease in both docosahexaenoic acid (DHA) and total amount of poly-unsaturated fatty acids (PUFAs) in the ID + im1000 group compared to the control group. Furthermore, the control group had a higher amount of n-3 fatty acids compared to both the ID and ID + im1000 group, and the ID group had a higher amount of n-6 fatty acids compared to the ID + im1000 and control group. The results of stereological counting of the hippocampus showed a larger amount of neurons in the dentate gyrus (DG) of the ID + im1000 groups compared to the ID group.

Conclusion: The deleterious effects of congenital ID can be reversed to some degree by administering iron isomaltoside 1000 during the window of opportunity. While motor defects and low hematological values resulting from congenital ID are reversed completely, the results suggest that the lipid composition of the cerebellum cannot be fully recovered to that of normal individuals. In addition, the results suggest that the amount of neurons in the DG can be improved by administering iron in early life.

_____

Marco Gall

TABLE OF CONTENT

INTRODUCTION

Iron is an essential micronutrient, characterized by its central role in the structure of hemoglobin and transport of oxygen to tissues. Moreover, iron is a necessary constituent of heme molecules, iron-sulphur proteins and iron-dependent enzymes, which are utilized in the majority of oxidative reactions in the mitochondrial respiratory chain([1]). In addition iron plays an important role in regulating cell mitosis in the DNA synthesis phase, by constituting a part of the enzyme ribonucleotide reductase, which catalyzes the conversion of ribonucleotides into deoxyribonucleotides([1]). Iron is also involved in central nervous system (CNS) processes ([2]) and is important in myelin synthesis and neurotransmitter metabolism([3]).
Iron deficiency is the most prevalent nutritional disorder, affecting approximately 25 % of the world's population, especially in developing countries ([4]). The prevalence of anemia among children younger than four years of age is estimated to range between 46 % and 66 % in developing countries, and half of the anemia cases are thought to be caused by iron deficiency anemia ([5]). Iron deficiency anemia, however, is not only a problem in developing countries. In industrialized countries the affected individuals are mostly infants, because of their high iron requirement during growth, and women of childbearing age, particularly pregnant women([6]).
Iron deficiency can have severe effects on both cognitive and physical development in children and on physical performance in adults ([7]). Early life iron deficiency affects specific brain areas undergoing development. This can have both short- and long-term consequences, where the damages are characterized by the onset, duration and severity of iron deficiency ([8]). Previously, it was thought that the deleterious effects of iron deficiency were mediated through anemia. It is now known that even a small decline in iron levels in the CNS, which does not necessarily lead to anemia, alters the cerebral energy metabolism([9]).

IRON METABOLISM

The amount of iron in the human body is approximately 3-4 g([10]). In healthy adults there is a daily loss of between 0.5 mg and 2.0 mg, due to the constant exfoliation of epithelial cells in the gastrointestinal tract, urinary tract, and on the integument ([11]). Hence, in order to maintain iron homeostasis, a daily dietary iron uptake is required.
Cellular iron import occurs in the proximal part of the small intestine, especially in the duodenum ([12]). Dietary iron is available in two basic forms: either bound to heme or in a non-heme form. Heme-bound iron is obtained from meat products, with a bioavailability of 20 % - 30 %, and non-heme-bound iron from vegetables, cereals and fruits with a bioavailability of 1 %- 10 %([10]). The non-heme iron that enters the duodenum is mostly available in the ferric form (Fe^{3+}), which is considered non-bioavailable. In order for the iron to be absorbed, it must be converted from Fe^{3+} to ferrous iron (Fe^{2+}). Several dietary components have such reducing capabilities, counting ascorbic acid([13, 14]) and amino acids such as cysteine([15]) and histidine([16]). Moreover, a study demonstrated that the brush border surface of duodenal enterocytes contain the enzyme duodenal cytochrome b (Dcytb), which possesses ferric reducing characteristics([12]). Subsequent to the reduction by either Dcytb or dietary components, Fe^{2+} is transported across the membrane of the enterocytes via the divalent metal transporter 1 (DMT1)([17]). Four isoforms of the DMT1 have been identified, of which one contains an iron responsive element and is considered to be the major functional isoform([18]). Additionally, it is suggested that the

low pH level in the proximal duodenum and the acidic microenvironment at the brush border, facilitate iron uptake across the membrane, by stabilizing the Fe^{2+} and by providing protons essential in transmembrane movement([11, 19]).

The mechanism behind absorption of heme iron is not fully understood. An early theory proposes that heme iron is absorbed via endocytosis as an intact molecule([20]). Supporting this hypothesis, a recent study demonstrated that duodenal enterocytes express high amounts of heme carrier proteins (HCP1) that seemingly are important for influx of heme molecules. However, the exact mechanism of HCP1 is still to be elucidated([21]).

Following absorption, heme can be detected in membrane-bound vesicles within the cytoplasm. In the vesicle, removal of iron from heme molecule occurs probably by interaction with heme oxygenase 1 (HO1). Fe^{2+} is then released into the cytoplasm, where it accumulates in a common intracellular pool([22]). If iron demand is low, a large amount of the accumulated iron is stored in intracellular protein complexes known as ferritin ([23]). Ferritin is able to store up to a few thousand iron atoms by binding otherwise toxic free Fe^{2+} to a ferroxidase site([23]). Fe^{2+} is then oxidized to Fe^{3+} and is aggregated in an iron core([25]). Due to the rapid turnover of enterocytes, ferritin is constantly lost into the intestinal lumen as aging cells are sloughed([24]). The continuous loss of ferritin is believed to be important for maintaining iron homeostasis by controlling the amount of iron exported to the circulation([24]). A simplified illustration of iron absorption and metabolism is showed in Figure 1([25]).

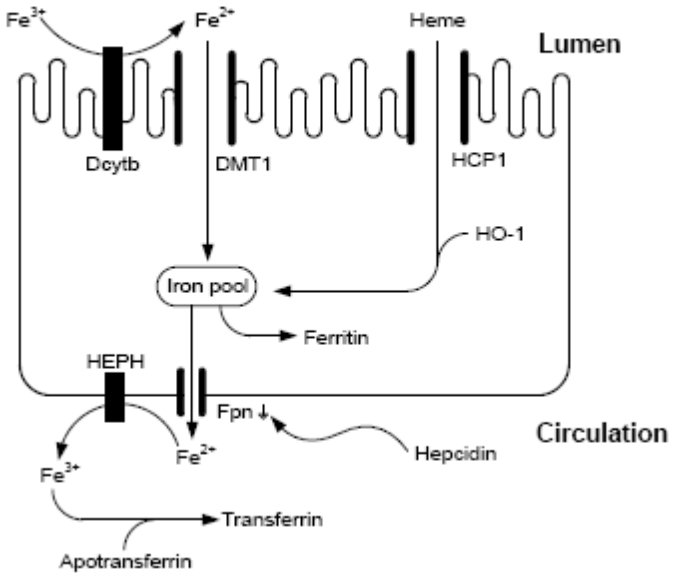

Figure 1: Non-heme iron is present in the lumen as Fe3+ and is reduced to Fe2+ by the enzyme Dcytb located on the brush border of duodenal enterocytes. Fe2+ is then transported into the cytoplasm by DMT1. Heme bound iron is transported to the cytoplasm via the carrier protein HCP1, whereupon the iron is stored in vesicles. The iron bound to heme is released by oxidation with HO-1. Free Fe2+ accumulates in a common pool and is stored by the intracellular protein ferritin. Fe2+ is exported out of the cell via Fpn. Before binding to the plasma protein, trans-ferrin, Fe2+ is oxidized to Fe3+, probably by the ceruloplasmin homologue, HEPH. Hepcidin is a liver derived hor-mone responsible for the internalization and degradation of Fpn. Dcytb: duodenal cytochrome b. DMT1: divalent metal transporter 1. HCP1: heme carrier proteins 1. HO-1: heme oxygenase 1. HEPH: hephaestin. Fpn: ferroportin. The illustration is modified from Anderson et al, 2009([25]).

Cellular iron export involves a two-step process, starting with ferroportin (Fpn) which transports iron to the basolateral surface of enterocytes, if iron demand is high([26]). If there is no demand for iron, Fpn is internalized and degraded by hepcidin, a hormone produced by the liver([27]). Before iron can be released from Fpn and bind to transferrin (Tf) it has to be oxidized by a ferroxidase to Fe3+ ([28]). Studies have demonstrated that in the intestine this oxidation is facilitated by the ceruloplasmin homologue hephaestin (HEPH)([29]). The oxidized Fe3+ binds to an iron-carrying plasma protein, apotransferrin, resulting in a conformational change to Tf, before being transported via the circulation to other tissues. Tf interacts with the transferrin receptor (TfR) on the cell membrane internalizing iron via endocytosis of the Tf–TfR complex([30]).

IRON CIRCULATION IN THE BRAIN

Iron bound to Tf is hydrophilic and is therefore unable to pass through the blood-brain barrier (BBB) passively ([31]). Hence, the brain acquires iron by expressing transmembranal TfR1, which can transport iron across the BBB ([32]) , on the luminal side of the brain capillary endothelial cells (BCECs). Although the iron uptake of the brain is predominantly achieved by TfR1 transport, a small amount of iron is taken up through the choroid plexuses.
The uptake of iron by the Tf-TfR1 complex is a multistep process starting with the attachment of Tf to the luminal segment of TfR1. The formed Tf-TfR1 complex is internalized by endocytosis and transported in an endosome. The endosomal environment is slightly acidic, thereby causing Fe^{3+} to disassociate from the Tf-TfR1 complex and reducing it to Fe^{2+}. The Fe^{2+} molecule is then liberated from the endosome by DMT1 and transported to the cytosol in exchange for two protons ([17]). The exact mechanism by which Fe^{2+} is transported from the cytosol in the BCECs to the extracellular fluid of the brain has not yet been discovered. It has, however, been proposed that Fpn transports the ferrous iron to the extracellular fluid ([33]). Once in the extracellular fluid, the Fe^{2+} ions are oxidized to Fe^{3+} by ceruloplasmin, which is expressed in astrocyte end-foot processes, and bound to apotransferrin. Alternatively the Fe^{2+} ions bind to ATP or citrate released from astrocytes and is transported in the form of non-transferrin-bound iron ([31]). After crossing the BBB, the iron is taken up by neurons for intracellular utilization. Neurons actively express DMT1 and TfR1. The TfR1 is up-regulated during ID ([34]), while the DMT1 remains unaffected by ID ([35]). Iron export from the neurons is actively regulated by Fpn, which is essential for maintenance of iron-homeostasis ([36]), and the iron is cleared from the brain parenchyma by reabsorption of cerebrospinal fluid from the subarachnoid space into the venous drainage system ([37]).

CONSEQUENCES OF IRON DEFICIENCY ON THE BRAIN

Aside from general symptoms caused by ID such as dizziness, paleness and fatigue ([38]), neurological symptoms are often exhibited in children with ID. Iron is utilized in synaptogenesis, neurotransmitter and fatty acid synthesis, myelination and as a cofactor to enzymes involved in brain development. Due to the unfavorable effects of ID on CNS development, such as reduced IQ ([5]) and abnormalities in structures associated with memory ([8]), it is crucial for the brain to acquire adequate iron supply during development ([39]).

MYELINATION

Oligodendrocytes are the cells in the CNS which stain most strongly for iron, even in CNS areas with high iron concentration such as the substantia nigra and the striatum ([2]). The role of oligodendrocytes is to produce myelin to insulate the axonal processes in the CNS, thus enabling salutatory conduction ([40]). Oligodendrocytes are the most metabolically active cells in the CNS and depend on abundant ATP supply. Iron is used as a cofactor to cytochrome A, B and C in the oxidative chain involved in ATP production. Hence, in cases of ID the ATP synthesis is impaired and the metabolic demand of oligodendrocytes is not met, leading to limited myelin production ([2]).
Cholesterol and lipid synthesis usually occur at a very high rate in the oligodendrocytes. Iron-dependent enzymes such as fatty acid desaturase and lipid dehydrogenase are normally present in oligodendrocytes in substantial amounts. However, under ID conditions the amount of iron-dependent enzymes decline leading to reduced oligodendrocyte functionality ([41]) and reduced myelin production ([42]).

SYNAPTOGENESIS

Synapses and dendrites are the main constituents of neuronal circuits. Synapses are subcellular junctional structures composed of a presynaptic terminal, a synaptic cleft and a postsynaptic target, which is normally a dendritic spine. The formation of synapses occurs by either formation of synaptic boutons along the axon shaft or at the end of axonal branches ([43]). Several neurotrophins, which play an important role in synapse and dendritic spine maturation, have been discovered, including brain derived neurotrophic factor (BDNF). BDNF regulates neurogenesis, neuronal survival, dendritic growth and plasticity across the entire life span ([44]).
Fetal and neonatal ID has been shown to lower the levels of BDNF mRNA expression in the rat hippocampus, suggesting that ID compromises synaptogenesis and alters the morphology of synapses and dendrites ([45]). However, ID induces an up-regulation of other neurotrophic factors such as glia-derived neurotrophic factor (GDNF), epithelial growth factor (EGF) and nerve growth factor (NGF), indicating a compensatory utilization of different signaling pathways in case of compromised BDNF signaling.
Dendritic arborization is important for neuronal plasticity and can be affected by several perinatal insults, one of which is ID. The cytoskeleton of the dendritic spines is composed of actin filaments, which are contractible, and therefore important for dendrite plasticity. The contraction of the actin filaments is a highly ATP-dependent mechanism and sufficient metabolic activity is required. Microtubule polymerization and microtubule associated protein-2-phosphorylation, which are involved in dendrite formation, are also highly ATP-dependent processes. Consequently, insufficient ATP production as a result of ID can alter dendritic structure and arborization ([46]).

MONOAMINE METABOLISM

There are many different monoamine neurotransmitters in the brain. ID affects the metabolism of several monoamines, however, the most studied and well documented monoamine affected by ID is dopamine (DA). DA is the predominant neurotransmitter of the mammalian extrapyramidal system and of several mesocortical and mesolimbic neuronal pathways ([47]). The receptors for DA (D1 and D2) are widely distributed in these areas, particularly in the striatum. The striatum is a part of the basal ganglia, a structure richly innervated by dopaminergic fibers which is associated with cognitive and

emotional processes, memory, motivational behavior and motor function. The amount of dopaminergic fibers in the striatum is closely correlated to the amount of iron. ([48])
Tyrosine Hydroxylase is a central iron-dependent enzyme in the synthesis of DA and norepinephrine (NE). Under ID the enzyme is not fully functional ([49]), leading to a decreased amount of intracellular DA. ID has the same effect on several other iron-dependent enzymes, such as tryptophan hydroxylase, which is responsible for the synthesis of serotonin (5-HT)([48]).
ID Influences the mechanism responsible for recycling the DA. The DA transporter (DAT) imports DA from the extracellular fluid to the presynaptic neurons, where it is stored in vesicles for later utilization. The mechanism of DAT is responsible for approximately 80% of the DA reuptake, however, under ID conditions the amount of DAT is reduced, leading to decreased reuptake of extracellular DA ([50]). There is a general consensus that the density of D2 is reduced in the striatum ([49, 51]), caudate putamen ([52]), and nucleus accumbens ([53]), which is often clinically related to abnormal locomotion ([52]).

Behavioral Alterations

Consequences of ID on the behavior of infants and children are often long-term. Several studies have shown that ID has a deleterious effect on intelligence and cognitive performance ([8]). It is estimated that IQ will decrease 1.73 points for each 10 g/L decrease in hemoglobin ([5]). Moreover, it has been observed that infants with ID are more hesitant and wary and less attentive than non-ID infants of similar age ([54]). Despite iron therapy, children with ID score lower on tests assessing mental, motor and social-emotional functioning, compared to non-ID children ([5]). The cognitive deficits of ID children have been shown to be long-term implications, lasting up to the age of 19 ([55]), and possibly further.

Fatty acids

Fat from dietary resources is primarily in the form of triglycerides; esters of glycerol and free fatty acids. The fatty acids (FAs) vary in chain length and in saturation. Saturated FAs, such as stearic acid, have only single bonds between atoms. Unsaturated FAs, however, contain one or more double bond. The hydrogen molecules related to the double bonds can be in the *Cis* or *Trans* position, most natural FAs being in the *Cis* position. Unsaturated FAs can be subdivided into monounsaturated FAs which contain one double bond, and polyunsaturated FAs (PUFAs), which contain more than one double bond.
Most FAs have a systematic name, which is a complete description of the structure of the FA, and a trivial name. The most often used descriptions of FAs are lipid numbers such as 18:2, the number on the left side of the colon indicating the number of carbon molecules while the number on the right side indicates the number of double bonds. The numbering of the systematic name usually starts at the carboxylic group of the FA, but on occasion it is better to number from the end methyl group. When numbering from the methyl group the numbers were prefixed with the Greek letter ω, but n- is now preferred to indicate the number of carbon molecules before the first double bond. See Table 1.

FA Structure	Trivial name	Systematic name	Lipid number
$CH_3(CH_2)_4CH=CHCH_2CH=CH(CH_2)_7COOH$	Linoleic Acid	Cis-9, Cis-12-octadecadienoic acid	18:2n-6
$CH_3(CH_2)_7CH=CH(CH_2)_7COOH$	Oleic Acid	Cis-9-octadecenoic acid	18:1n-9
$CH_3(CH_2)_{16}COOH$	Stearic Acid	Octadecanoic acid	18:0

Table 1: The structure, trivial name, systematic name and lipid number is shown for a poly-unsaturated fatty acid (Linoleic acid), a mono-unsaturated fatty acid (Oleic acid) and a saturated fatty acid (Stearic acid)

Some PUFAs are essential FAs (EFAs), meaning that the human body is unable to synthesize them so they must be acquired from dietary sources ([56]). Under normal dietary circumstances the EFAs consist of α-Linolenic acid (ALA, C18:3n-3) and linolenic acid (LA, C18:2n-6). However, in cases of ALA and LA deficiency, the body is unable to synthesize long-chain derivatives of before-mentioned PUFAs, which therefore also become EFAs.

FATTY ACIDS IN THE BRAIN

The most assiduously studied PUFAs are the n-3 and n-6 PUFAs which have been shown to have a neuroprotective effect against both age-related loss of cognitive function ([57, 58]) and Alzheimer's Disease ([59]). PUFAs constitute a high amount of the FAs in the CNS ([60]) and play a large role in the development and function of the human brain ([56]). Long-chain PUFAs (LC-PUFAs) in particular, such as docosahexaenoic acid (DHA, C22:6n-3) and arachidonic acid (AA, C20:4n-6), are involved in neuronal processes such as maintenance of membrane fluidity and regulation of gene expression ([56]) and DHA is critical for the optimal function of the retina ([61]). N-6 and n-3 PUFAs are essential for development and maintenance of normal brain and nervous system function throughout the entire life span ([62]) and deficiencies or imbalances between these essential PUFAs has been theorized to cause behavioral, neurological or psychiatric disorders in both children and adults, although evidence is too limited to reach a definitive conclusion. ([63]).
Mammals are unable to synthesize the parent molecules of both n-3 and n-6 PUFAs, ALA and LA, respectively. The long-chain derivatives of ALA and LA can be synthesized by means of a multistage conversion process (Figure 2) which takes place in the endoplasmatic reticulum of the liver cells ([64]).

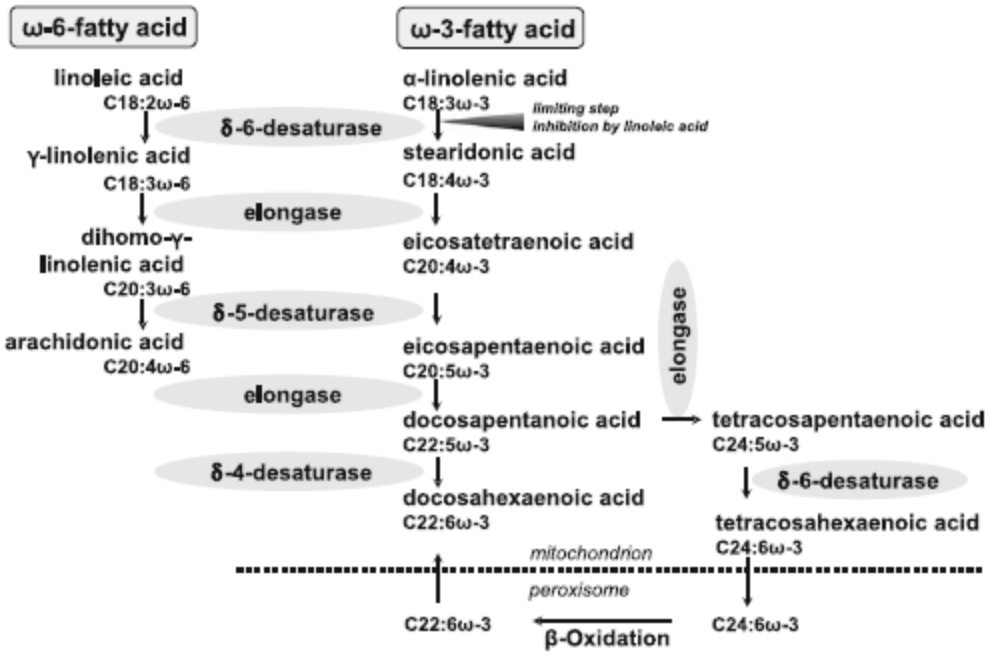

Figure 2: The conversion process of ALA and LA in the endoplasmatic reticulum of the liver: Through a series of elongations and desaturations, facilitated by the enzyme-families Desaturase and Elongase, the LA and ALA PUFAs are converted into AA and DHA, respectively, which have longer carbon chains and are metabolically active. The n-6 and n-3 PUFAs compete for the enzyme systems. This conversion process is extremely unyielding ([65]), thus proving the need of dietary intake of LC-PUFAs.

THE HIPPOCAMPUS

The hippocampus belongs to the limbic system and is a major component of the brains of humans and other mammals. The hippocampus is a paired structure which in primates is located in the medial temporal lobe, beneath the cortical surface (Figure 3).

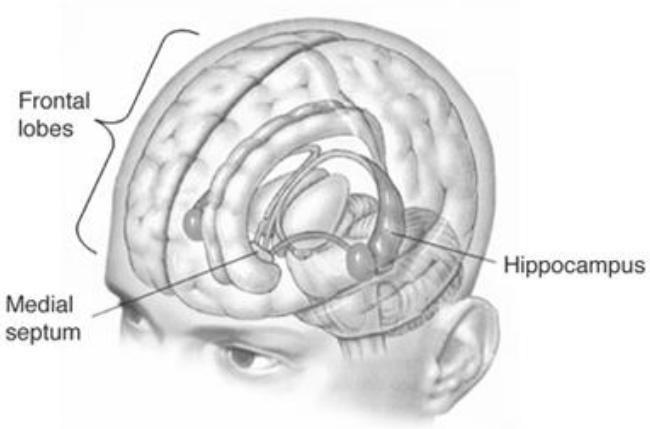

Figure 3: Drawn image of the human brain showing the location of the hippocampus, in the medial temporal lobe (picture acquired from www.brainmind.com(2011)).

The hippocampal formation is constituted by three parts; the dentate gyrus (DG) Ammon's horn (CA) and the subiculum. When observing a hippocampus which has been cut horizontally, the DG and CA appear as two interlocking C's. The CA is subdivided into three regions; CA1, CA2 and CA3.
CA1, which is also known as regio superior, consists of small, tightly packed nuclei with small nucleoli in layers about 4-5 cells deep ([66]). The cells in regio superior become more loosely packed toward the subiculum, and the border between regio superior and subiculum is defined as the point at which the superficial cells of regio superior cease to be continuous ([66]).
CA2 and CA3 are often counted together, since the cells in CA2 are recognizable only if a golgi-staining procedure is used ([67]). CA2/3, also called regio inferior, has larger nucleoli than regio superior and irregular nuclei with an ovoid shape. The nuclei in regio inferior are loosely packed in layers of 6-7 cells.
The DG consists of granular cells as opposed to the CA areas which consist of pyramidal cells. The granular cells in the DG are small, tightly packed and arranged in layers of approximately 8-15 cells ([66]).

THE HIPPOCAMPAL CIRCUIT

The hippocampus is part of an organized system of structures in the temporal lobe which is important in forming long-term memory ([68]). The hippocampus receives highly processed information from widespread neocortical regions through three temporal cortical areas; the entorhinal, perirhinal and postrhinal cortices. The entorhinal cortex can be viewed as the main relay station for sensory information. The major input from the entorhinal cortex to the hippocampus comes from layer II of the entorhinal cortex and forms part of the perforant pathway. This projection provides a great input to the DG, which in turn provides the major input to CA3 through mossy fiber projections. CA3 provides input to CA1 through the Schaffer collateral pathway, although there is a large recurrent associational projection back to CA3. CA1 primarily projects to the subiculum which largely projects to the entorhinal cortex layers IV and V. From here the information is sent to widespread neocortical areas. (Figure 4)

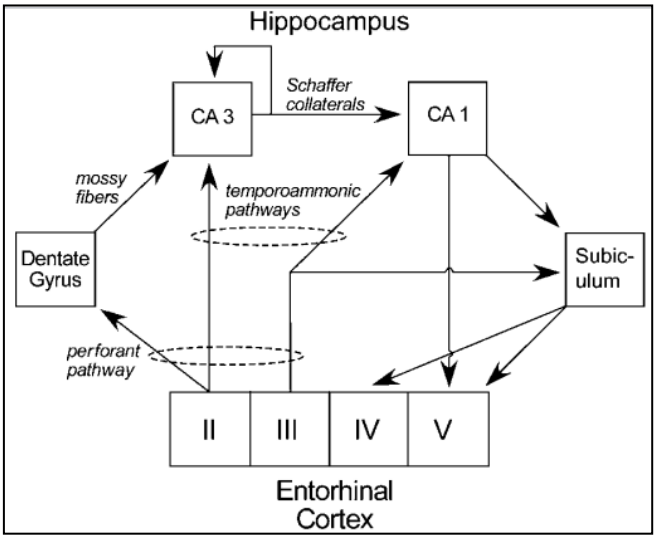

Figure 4: Simplified schematic of the hippocampal circuit. The path of sensory information travels from the neocortex to the entorhinal cortex, which relays the information to the DG which projects the information to CA3 which again projects to CA1.

CA1 and subiculum can receive information directly from the entorhinal cortex, and send information to the entorhinal cortex, from which it is sent to the neocortex. ([68])

HIPPOCAMPAL FUNCTION

There is a general consensus that the hippocampus is involved in memory and learning, although the exact function is much debated. In addition, several studies have shown that conditions which negatively affect adult neurogenesis in the rodent DG, such as stress and aging, impair learning ability ([69,70]). Magnetic resonance imaging studies have shown a decreased hippocampal size in patients suffering from depression ([71]), suggesting that the hippocampus is involved in mood disorders. It has been proposed that this decrease in hippocampal size is caused by reduced neurogenesis, and that the efficacy of antidepressants lie in their ability to restore neurogenesis to normal levels.
Another role of the hippocampus is that of a stress regulator. The hippocampus has a high concentration of adrenal steroid receptors ([72]) and direct projections to the hypothalamus ([73]) which provides a link between the hippocampus and the regulation of the stress response. Evidence of the role of hippocampus as a negative feedback regulator of the HPA-axis is found in studies demonstrating that destruction of the hippocampus prevents efficient cessation the HPA-axis, while stimulation of the hippocampus reduces stress-induced HPA-axis activation ([73]).

METHODS

ANIMALS AND DIET

During the experiment rats had access to water and food *ad libitum.* They were housed in 48cm x 37.5cm x 21cm cages (1500U Eurostandard Type IV S, Scanbur A/S, Karlslunde, DK) at the Animal Department of Aalborg Hospital, Aalborg, DK. The rats were housed under constant temperature and humidity conditions, and kept on a 12 hour light/dark cycle. All procedures concerning animals in this study were approved by the Danish Experimental Animal Inspectorate under the Ministry of Justice. Female rats (n=14) of the Wistar strain (age: 12 weeks) were purchased from a commercial supplier (Taconic, Ry, DK) and kept on a normal diet (1214 FORTI breeding diet, Altromin Spezialfutter, DE) the first week after arrival. The rats were then placed in individual cages, composed of a plastic bottom and sealed with a metal lid. Cages were filled with a layer of sawdust, a small pile of hay for nesting material and a transparent red cylinder. A week after arriving, the rats were weighed (240g – 260g). The rats were randomly assigned into an iron deficient (ID) group (n=9) and a control group (n=5). Iron deficiency was induced by collecting 2.0mL (equaling ~1% of total body weight) of blood. This was done by anaesthetizing the rats with Hypnorm (0.315 mg/ml fentanyl citrate, VetaPharma, UK) – Dormicum (5 mg/ml, Hameln Pharmaceutical, Gloucester, UK) diluted in a saline solution (mixture proportion: 1:1:2), at a dose of 0.15 – 0.2 ml per 100g. Afterwards blood was either collected by left ventricle heart puncture (n=8) or by venous puncture of the tail (n=2). One rat died following the heart puncture and was replaced by a rat from the control group. To maintain iron deficiency the ID rats received a special controlled diet low in iron (<10mg/kg) (C 1038 iron deficient diet, Altromin Spezialfutter, DE), whereas control rats were kept on a normal diet. Two days post blood collection, female rats (n=13) were mated with male Wistar rats (n=13) fed a normal diet. Male rats were placed with female rats for 8 days to ensure pregnancy.

OFFSPRING

The offspring (n=174) was born after approximately three weeks of gestation. ID rats (n=9) gave birth to 122 pups (12-15 pups/litter), whereas the control rats (n=4) gave birth to 52 pups (10-15 pups/litter). Dams with matching pups were divided into 3 groups:

1. Iron deficient pups receiving saline (ID) (n=68).
2. Iron deficient pups receiving iron isomaltoside 1000 (ID + im1000) (n= 54).
3. Iron sufficient pups receiving saline (control) (n=42)

IRON INJECTIONS

Iron isomaltoside 1000 (PharmaCosmos, Holbaek, DK) was diluted in a saline solution and given as subcutaneous neck injections in the ID + im1000 group. Injections of iron isomaltoside 1000 began at P1-P4 at a dose of 45mg Fe/kg body weight. Rat pups in the ID and control group were injected with saline solution instead of iron isomaltoside 1000 from P3-P6. Injections and weight measurements were carried out every 3-4 days.

HCT MEASUREMENTS

To assess the degree of ID in the animals, blood was taken in order to determine their Hct-values, which is directly correlated to ID.
Four random female pups (P8-P13) from the ID, ID + im1000 and control group were euthanized by decapitation to gain enough blood for Hct analysis. Trunk blood was collected in heparinized capillary tubes and used for Hct measurement. 2-3 samples were collected from each rat pup. The samples were centrifuged (Mikro 12-24, Andreas Hettich GmbH & Co. KG, Tuttlingen, DE) for 5 minutes, and the Hct values measured on a micro-hematocrit reader (Adams Micro-Hematocrit reader, Clay Adams, New Jersey, USA).
Approximately one week later, four additional random female pups (P15-P18) from the ID, ID + im1000 and control group were weighed and anesthetized by intraperitoneal injection of Hypnorm – Dormicum diluted in a saline solution (mixture proportion: 1:1:2), at a dose of approximately 0,1 ml. Blood was collected from the right atrium and stored in heparinized capillary tubes for Hct measurements. At P86-94, when the rats were euthanized, another batch of blood was collected from female ID (n=11), ID + im1000 (n=11) and control (n=20) rats.

FOOTPRINT ANALYSIS

The test was performed on male rats (n=10, P85-P90) from each group. The hind limbs of the rats were dipped in non-toxic blue ink and placed in a 40 cm long black tube covered with a paper strip (approximately 8 cm wide and 46 cm long), see Figure 5. The narrow tube ensured that the rats walked in a straight path. If a rat stopped in the middle of the tube, or refused to enter the tube, the session was repeated. For inter-limb coordination the distance between the center pads of the ipsilateral hind feet was measured. Moreover, the distance between center pad of the right and left paw was measured to evaluate the stability of the gait.

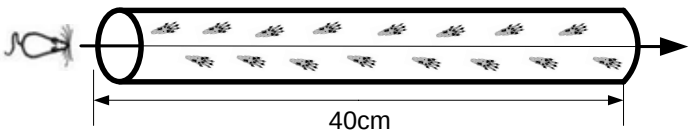

Figure 5: Illustration of the footprint analysis.

TISSUE COLLECTION

Rats were randomly assigned to either fixation/stereology (n=41) or biochemical analysis (n=18) at P86-P94.

The rats were given a high dose of Hypnorm–Dormicum diluted in saline solution. When they reached unconsciousness, the ribcage of the rats was excised. The rats for stereology (n=41) were injected with 40mL saline into the left ventricle to rinse the blood vessels, prior to a 50mL 4% paraformaldehyde injection. Right liver lobe, spleen, right kidney, stomach, duodenum, femur, right eye and the brain was dissected and stored in 50mL nunc tubes containing 4% paraformaldehyde. After approximately 24 hours, the organ samples were placed in potassium phosphate buffered saline (KPBS) (149mmol NaCl, 2mmol KCl and 4.9% PBS). Sodium azide (NaN_3) was added to avoid decomposition of the tissue. The brains were then dissected in order to provide the hippocampus of one hemisphere for stereology. The brain was parted along the sagittal sulcus and the cerebellum was excised and the forebrain was parted by making an incision directly anterior to the optic chiasm. Thereafter a horizontal incision was made inferior to the corpus callosum in order to yield two halves containing hippocampus.
The rats (n=18) used in the biochemical analysis were anaesthetized, decapitated and the brain was removed from the cranium, along with the duodenum and right liver lobe and quickly stored on dry ice in 50mL nunc tubes. The organs were subsequently stored at -80°C.

TOTAL IRON CONTENT

Inductively Coupled Plasma Mass Spectrometry (ICP-MS) was used to determine differences in the total amount of iron between the groups. The mesencephalon from the ID (n=5), ID + im1000 (n=6) and control (n=7) groups were weighed and thereafter placed in MF100 vessels (Anton Paar, Graz, AT) along with 2 ml MilliQ H2O, 2 ml 67.5 % HNO3 and 200 µm 10 ppm yttrium (1 ml yttrium, 20 ml 67.5 % HNO3 and 79 ml MilliQ H2O). The MF100 vessels were then microwaved in a Multiwave 3000 (Anton Paar, Graz, AT) in 3 stages: Warming up to 1200 watt for 10 minutes, warming for 10 minutes at 1200 watt and a cool-down stage which lasted 15 minutes. The tissue was transferred to measuring tubes, filled to 10 ml with MilliQ H2O, and subsequently transferred to tubes used for ICP-MS. A metal standard consisting of Cu, Zn and Fe solutions of 1000 ppb, 100 ppb and 10 ppb respectively, was prepared by adding 5 ml, 0.5 ml and 0.05 ml of a 10000 ppb stock solution (0.5 ml Cu, 0.5 ml Zn, 0.5 ml Fe and 10 ml HNO3 and 38.5 ml MilliQ H2O) to 10ml HNO3 and filling up to 50 ml with MilliQ H2O. ICP-MS was carried out on all tissue samples (n=18) for approximately 45 minutes with an ICAP 6000 series (Thermo Scientific, Slangerup, Denmark) and the results were obtained from iTEVA ICP software (Thermo Scientific, Slangerup, Denmark).

FIXATION OF TISSUE

The fixated brains were pre-infiltrated in equal parts of 96 % ethanol and base liquid Technovit 7100 (Heraeus Kulzer GmbH, Wehrheim, DE) at room temperature for 2 hours. After pre-infiltration the solution was replaced with an infiltration solution consisting of 100mL base liquid Technovit 7100 with added 1g Hardener I (Heraeus Kulzer GmbH, Wehrheim, DE). The tissue was infiltrated for 10 days at 4˚C. After 10 days of infiltration, embedding took place. 1mL of hardener II (Heraeus Kulzer GmbH, Wehrheim, DE) was added to 15mL of the infiltration solution. 1-3mL of the embedding solution was applied into the bottom of a plastic Histoform S (G3754 1.3cm x 1.9cm x 5cm Mould tray, Axlab, Vedbæk, DK) and placed at 40˚C for one hour until the solution had solidified. The infiltrated specimens (systematically selected from either the left or right hippocampal formation) were placed in the histoforms, positioned with the cutting edge facing downwards and filled with approximately 1mL

embedding solution. An adaptor was placed on top of the embedding solution and the mold was allowed to congeal for 24 hours at room temperature.

SLICING

The molds were positioned on a microtome (Finesse® 325, Thermo Shandon, Pittsburgh, PA) and trimmed. When reaching the hippocampus formation, the tissue was brushed with water for approximately 40 seconds before 40µm thick sections were cut. With a random starting point every sixth section was collected for analysis along with a back up section. The gathered tissue sections were placed in water and positioned onto SuperFrost glass slides (Hounisen laboratorieudstyr, Risskov, DK). The glass slides were covered with plastic with a weight on top and allowed to dry overnight at 60˚C.

STAINING

The sections were placed in a giemsa working solution (10mL giemsa stock solution, 40mL distilled water and two drops of 1% acetic acid) for 70 minutes. The sections were then transferred to a 1% acetic acid solution for 3 minutes and afterwards respectively put into 96% ethanol and 99% ethanol for 10 minutes each. The sections were briefly dipped in distilled water and allowed to dry overnight at 60˚C covered with plastic with a weight on top.

STEREOLOGICAL COUNTING

Counting of neurons in the hippocampus formation was performed using the newCAST software (Visiopharm, Hørsholm, DK). The stereological analysis system consists of an Olympus light microscope (Olympus BX51, Olympus, DK) modified for stereology with a digital camera (ColorView I, soft Imaging System, Münster, DE) and a motorized microscope stage (Prior H138 with controller H29, Cambridge, UK). The newCAST software is interfaced to the digital camera superimposing the counting frames on the live images. Stereological counting was performed on systematically selected tissue sections from each rat. The areas of hippocampus (CA1, CA2/CA3, and DG) were determined with a 100× oil immersion lens and masks were applied to specify the counting areas, see Figure 6.

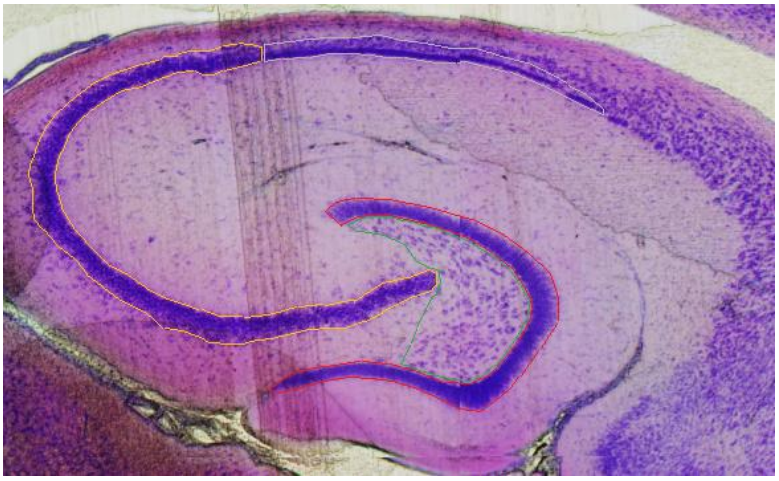

Figure 6: Hippocampus (-5.10 from bregma) with the three areas marked: Dentate gyrus (red), CA2/CA3 (orange) and CA1 (grey)

To estimate the total number of cells in the different counting areas, a systematic randomly sampled set of counting spaces was made. The quantity of counting spaces in each counting area was determined by the total size of the area. Further, identical distance between counting spaces, in the x and y direction, were defined by a chosen step length (defined by previous studies) (DG: 125, CA2/CA3: 100 and CA1: 70), see Figure 7.

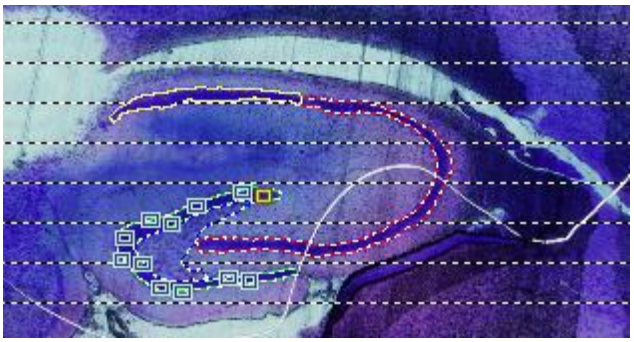

Figure 7: Systematic randomly sampled set of counting spaces in the dentate gyrus.

Inside each counting space, the optical dissector was applied. The optical dissector is a 3-D counting probe indicated by a counting frame. Each counting frame was composed of an inclusion (green line) and exclusion line (red line), see Figure 8. The size of the counting frame was determined by the density of neurons in the counting area. Cell counting was made with a 100× oil immersion lens using the nucleolus as the counting unit. Neurons were counted if they came into focus, within a fixed height of 20µm, inside the counting frame without touching the exclusion line. The dissector height is smaller than the section thickness, because of the potential bias from lost caps which is avoided by having upper and lower guard heights.

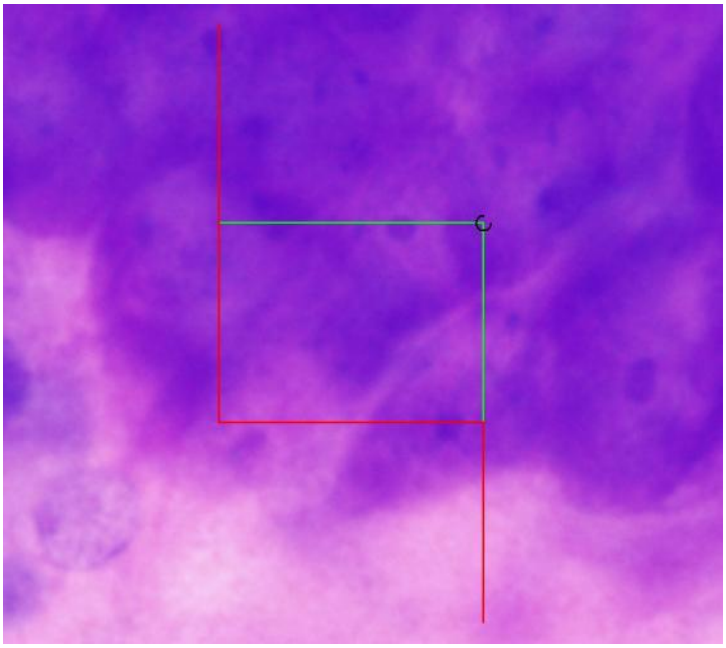

Figure 8: Counting frame in the CA1 area of hippocampus. The red line indicates the exclusion line, and the green line is the inclusion line. In this image only one cell would be counted.

ESTIMATION OF TOTAL CELL NUMBER

As the stereological counting only represents an estimate of the total number of neurons in each counting area of the hippocampus, a calculation was made to determine the total number. The formula used for the calculation: $N= \Sigma Q \times 1/ssf \times 1/asf \times 1/tsf$
The total number of neurons in the counting area (N) was calculated by knowing the section sampling fraction (ssf), the area sampling fraction (asf), the tissue sampling fraction (tsf) and the sum of all neurons found by stereological counting in each counting area (Q).
The section sampling fraction is the number of sections examined, so if every 6^{th} sample is examined the section sampling fraction would be 1/6. The area sampling fraction is how much of each section area is sampled. This is calculated by dividing the area of the frame, a, with the area associated with each x,y movement, A [asf =a(frame)/A(x, y step)]. The tissue sampling fraction is calculated by dividing the sampling height by mean section thickness.

FREE FATTY ACID ANALYSIS

The amount of different free fatty acids (FFA's) in the phospholipid groups; Phosphatidylethanolamine (PE), Phosphatidylserine (PS), and phosphatidylinositol (PI), was determined by extracting the lipid from the cerebellum of the animals, separating the phospholipid groups by thin layer chromatography (TLC), methylating the lipids and analyzing them by gas chromatography (GC).
Half of the cerebellum from 5 ID, 6 ID + im1000 and 7 control animals was used for this analysis.
The cerebellum halves, which had previously been excised and stored at -80°C, were weighed and transferred to 15mL round-bottom tubes. 7.5mL Chloroform:Methanol (2:1) was added and the tissue was homogenized for three times 10 seconds with 50 second intervals at ~20000rpm with a Polytron PT 2100 homogenizer. Afterwards the homogenized tissue was filtered through a glass funnel with a

paper filter into a 25mL measuring cylinder. The knife used for homogenization was rinsed with Chloroform:Methanol (2:1) and filtered through the same filter into the measuring cylinder.
0.73% NaCl at 0.2 times the volume of the sample was added to the extract in the measuring cylinder, which was shaken and placed at 5˚C overnight for phase separation. The top phase, consisting of water and proteins, was removed with a glass pipette and discarded. The bottom phase was transferred to a glass tube and the measuring cylinder was rinsed with 2.5mL Methanol which was also transferred to the glass tube. The bottom phase was desiccated with nitrogen gas for approximately two hours, and subsequently liquefied in approximately 1-1.5mL Chloroform:Methanol (95:5), in order to yield a concentration of about 20mg lipid/mL, and thereby prepared for phospholipid separation.
In order to ensure saturation of the saturation chamber, solvent, consisting of Chloroform:Methanol:Acetic acid:Water (70:30:12:4), was made the day before use and put in the chamber.
The preparative silica coated TLC-plates were etched with a sharp object in order to attain three lanes for each sample and one lane for the external standards. 50µL of the dissolved extract was applied on a TLC plate in wide bands 1.5cm from the bottom. Three extract bands along with four standard dots of 10µL each were placed on the same TLC plate, which was developed in a saturated chamber for 1.5hours. After drying the solvent on the TLC plate the lipids were sprayed with 2,7-dichlorfuorescin (0.2 % in ethanol) which was allowed to dry, and then visualized under UV-light.
Pentadecanoic acid at a concentration of 1mg/mL was applied on each of the four phospholipid groups as an internal standard. Due to the different concentrations of the phospholipid groups, 40µL pentadecanoic acid was applied on PE, while only 10µL was applied on PI and PS. The separated phospholipids were then scraped off, and placed in separate methylation-tubes.
The phospholipids were dissolved in 1mL 0.5N NaOH in Methanol and heated at 80˚C for five minutes after which 1mL 20% BF_3 in methanol and 0.5mL 0.1% hydroquinone in methanol was added and the samples were heated for additional two minutes. After cooling down for two minutes, 2.5mL Heptane and 2.5mL methanol:water (90:10) was added, and the glass tube containing the sample was vortexed for about ten seconds. The clear top layer was carefully removed with a pipette and stored in another glass tube. 2.5mL Heptane was added to the sample once more and the top layer was carefully removed and stored in before-mentioned glass tube. The new glass tube, containing clear liquid was dried under nitrogen gas for about 45 minutes and was thereby ready for GC analysis. The derivatized extracts were analyzed with an Agilent 6890 gas chromatograph coupled with an Agilent 5973 mass-selective detector (Agilent technologies, Santa Clara, CA, USA). 1-µl aliquots of the extracts were injected into a capillary column (SP-2380, 60 m × 0.25 mm i.d.; Supelco Inc., Bellefonte, PA). The MSD ChemStation software (G1701DA, Agilent technologies, Santa Clara, CA, USA) was used for processing of the data.

STATISTICS

The software application PASW Statistics 18.0 (SPSS Inc., Chicago, USA) was used for statistic analysis, along with Microsoft Excel 2007 (Microsoft, Redmond, USA). PASW Statistics 18.0 was used to calculate means, significant differences, standard error of mean (SEM) and produce statistical illustrations. Microsoft Excel 2007 was mainly used for organizing data from trial protocols.
To test for significant difference in a variable between two populations, several factors must be considered, before deciding which test to use. The samples must first be examined for Normal

distribution. This was done by evaluating histograms, Q-Q plots and performing Shapiro–Wilk test for normality. If the data were normally distributed, One-way ANOVA was used.
If the data was not normally distributed, a non-parametric test (Kruskal-Wallis One-way Analysis of Variance) was used. The significance level in this study was set to $\alpha=0.05$ ($p=0.05$).

RESULTS

HEMATOCRIT

Hct values were obtained three times during the experiment. First measurement on rat pups at P8-P13, second at P15-P18 and third on the adult rats at P86-P94. Exact mean values are listed in Table 2. Values from the first Hct measurement (P8-P13) are illustrated in Figure 9. ID rats had a mean Hct value of 14.18% ±0.79 and control rats had a mean Hct value of 31.50% ±1.02, see Table 2. Thus, ID rats had a 54.98% smaller Hct value than control rats. The results showed that ID rats had a significant lower Hct compared to both ID + im1000 (p=0.034) and control rats (p=0.032), see Figure 9.
Values from the second Hct measurement (P15-P18) are illustrated in Figure 10. ID rats had a mean Hct value of 10.31% ±0.72 and ID + im1000 rats had the highest mean Hct value at 30.12% ±0.56, see Table 2. Thus, ID rats had a 65.77% lower Hct value than ID + im1000 rats. The results showed that ID rats still had a significantly lower Hct value compared to both ID + im1000 (p=0.021) and control rats (p=0.020), see Figure 10.

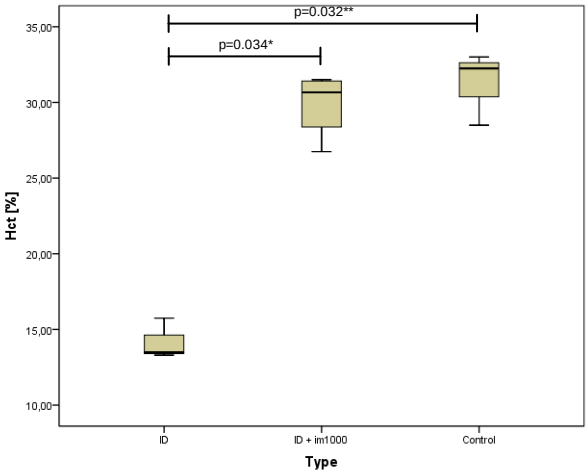

*Figure 9: Boxplot of the first Hct measurements at P8-P13. The mean of 1-3 measurements per rat (n=11) is grouped by type. ID (n=3), ID + im1000 (n=4) and control (n=4). *Significant difference between ID rats and ID + im1000 (p=0.034). **Significant difference between ID rats and control rats (p=0.032). ID: Iron deficient.*

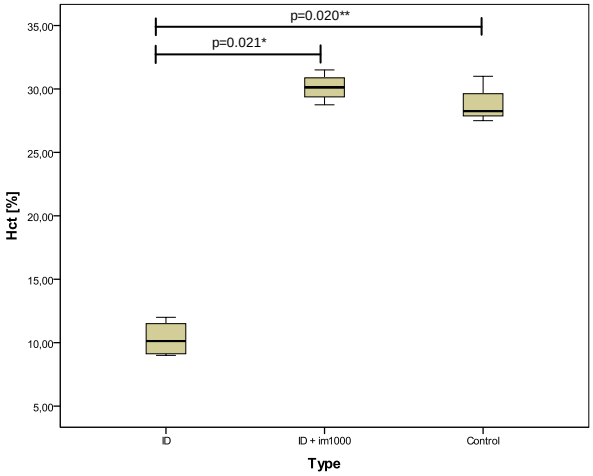

*Figure 10: Boxplot of the second Hct measurements P15-P18. The mean of 1-2 measurements per rat (n=12) is grouped by type. ID (n=4), ID + im1000 (n=4) and control (n=4). *Significant difference between ID rats and ID + im1000 rats (p=0.021). **Significant difference between ID rats and control rats (p=0.020). ID: Iron deficient.*

The third Hct measurements (P86-P94) were obtained when the male rats were sacrificed. The results are illustrated in Figure 11. Again, the lowest mean Hct value was observed in ID rats, with a mean value of 21.90% ±0.59 while the ID + im1000 rats had the highest mean Hct value of 44.00% ±0.49. Thus, the Hct value was 50.22% smaller than the ID + im1000 Hct value. Results showed that ID rats had significantly lower mean Hct than both ID + im1000 rats (p<0.000) and control rats (p<0.000). Furthermore, the results showed that ID + im1000 rats had a significantly higher mean Hct than control rats (p=0.014).

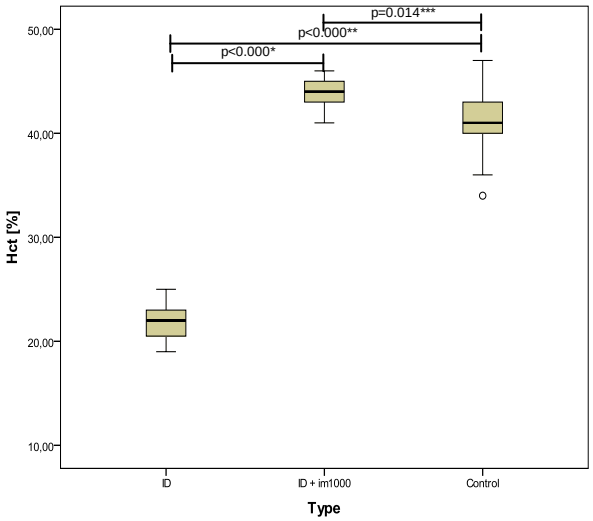

*Figure 11: Boxplot of the third Hct measurements at P86-P94. The mean Hct of the rats is grouped by type ID (n=11), ID + im1000 (n=11) and control (n=20). *Significant difference between ID rats and ID + im1000 rats (p<0.000). **Significant difference between ID rats and control rats (p<0.000). ***Significant difference between controls and ID + im1000 rats (p=0.014). ID: Iron deficient.*

Table 2: Mean hematocrit values [pct]. 1st at P8-P13, 2nd at P15-18 and 3rd at P86-P94

Type	1st mean*	2nd mean*	3rd mean*
ID	14.18 ±0.79 (n=3)	10.31 ±0.72 (n=4)	21.91 ±0.59 (n=11)
ID + im1000	29.90 ±1.10 (n=4)	30.13 ±0.56 (n=4)	44.00 ±0.49 (n=11)
Control	31.50 ±1.02 (n=4)	28.75 ±0.77 (n=4)	41.15 ±0.70 (n=20)

** Mean is stated with± SEM*

The progression of the mean Hct values is showed in Table 2 and Figure 12. There is a decline in mean Hct from P8-13 to P15-P18 in both ID and control rats, whereas ID + im1000 remain unchanged. From P15-P18 to P86-P94 there is an increase in mean Hct for all groups.

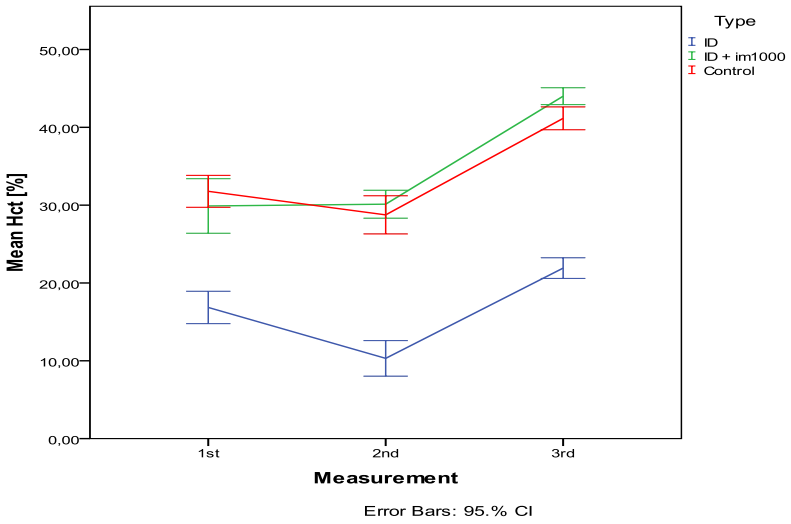

Figure 12: Hct values from the 1st, 2nd and 3rd measurements, along with a 95 % confidence interval. ID: Iron deficient.

Blood samples taken at P15-P18 are photographically illustrated in Figure 13. The blood samples from the ID rats were a brighter shade of red compared to the samples from both the ID + im1000 and the control rats.

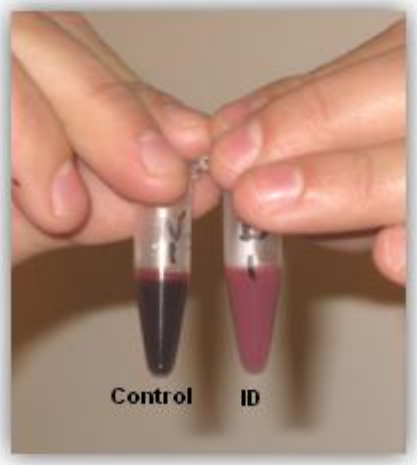

Figure 13: Blood samples from a control rat (left) and an ID rat (right) at P15-P18. ID: Iron deficient

FOOTPRINT ANALYSIS

The footprint analysis was performed at P85-P90 on rats (n=10) from each group in order to assess differences in balance and motor ability between the groups.
The distance between the center pads of the ipsilateral hind feet was measured. There were no significant differences in stride length of either leg between the groups, see Figure 14.

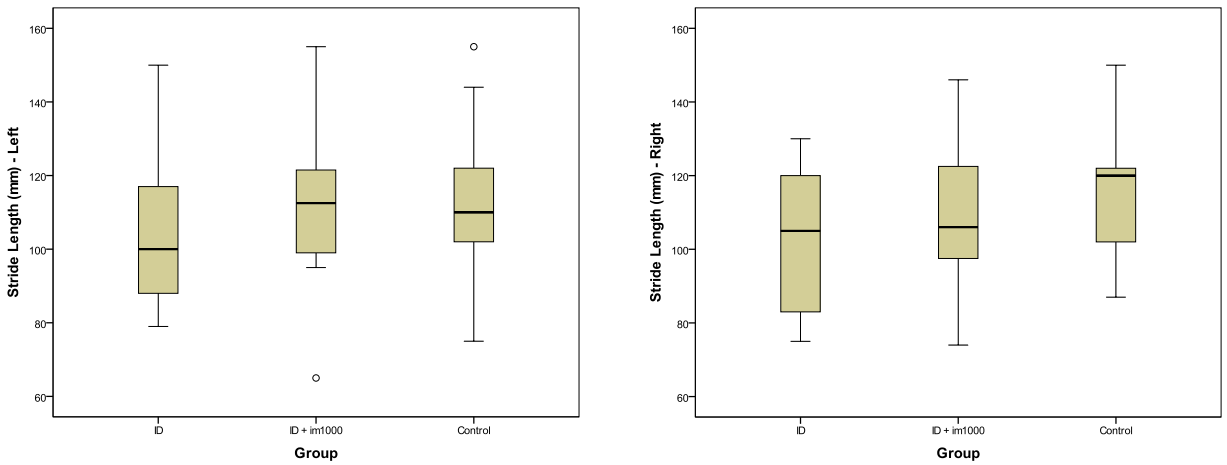

Figure 14: Boxplots of the stride length of both left and right foot, in the different groups. ID: Iron deficient

Analyses were made on gait width, to evaluate the stability of the gait. The distance between center pad of the right and left paw was measured. Results showed that ID rats had a significantly larger gait width compared to both ID + im1000 ($p<0.000$) and control rats ($p<0.000$), see Figure 15.

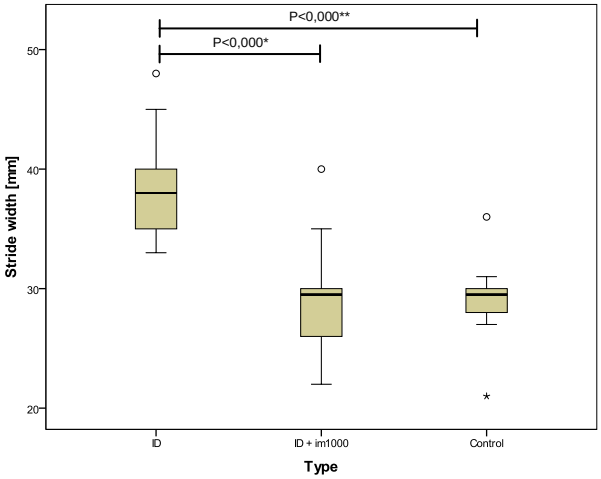

*Figure 15: Boxplot of the footprint analysis. The gait width for each rat (n=30, P85-P90) is illustrated and grouped by type. ID (n=10), ID + im1000 (n=10) and control (n=10). *Significant difference between ID and ID + im1000 rats (p<0.000). **Significant difference between ID and control rats (p<0.000).*

TOTAL IRON CONTENT

Total iron measurements were conducted on the mesencephalon. The analysis were made on rat brains from all groups, ID (n=5), ID + im1000 (n=6) and control (n=7). The mean iron amount is illustrated in both Figure 16 and Table 3. The lowest amount of iron was discovered in the ID group with a mean of 13.73 µg Fe ±1.58. The highest amount of iron was found in the control group with a mean of 25.33 µg Fe ±1.35. Statistical comparisons between the groups were made. The results showed that ID rats had a significantly lower amount of iron compared to the rats in the other groups; ID + im1000 (p=0.009) and control rats (p<0.000).

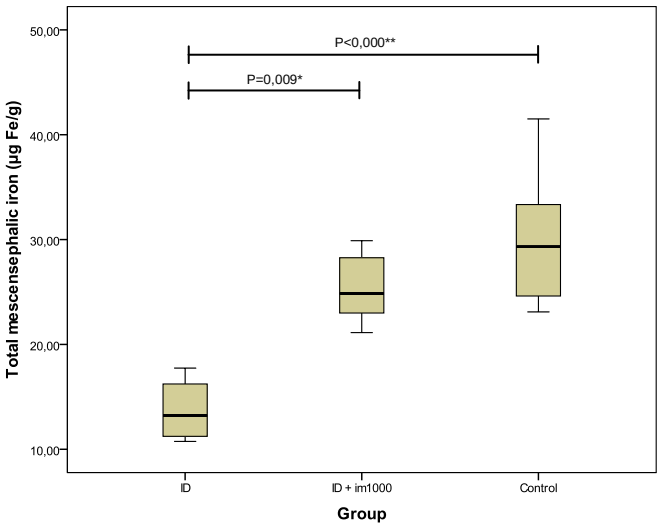

*Figure 16: Boxplot of the difference in total mesencephalic iron (µg Fe/g) between the groups.*Significant difference between ID and ID + im1000 (p=0.009). **Significant difference between ID and control rats (p<0.000). ID: Iron deficient.*

Table 3: total mesencephalic iron.

Type	Total mesencephalic iron (µg Fe/g) *
ID	13.73 ±1.58 (n=5)
ID + im1000	25.33 ±1.35 (n=6)
Control	29.98 ±2.52 (n=7)

** Mean is stated with± SEM*

STEREOLOGIC COUNTING

Stereologic counting of neurons in the hippocampus was performed on animals from the control group (n=2), the ID + im1000 group (n=8) and the ID group (n=3). The results from the three groups were compared for each hippocampal area which was counted. The mean number of neurons in the DG area of the hippocampus in the control group was 534,324.9 ± 72,740.7 while it was highest in the ID + im1000 group (679,380 ± 34,438.2). The ID group had the lowest mean number of neurons at 494,055.9 ± 26,954.3. The mean number of neurons in the CA2/3 area of the control group was 180,498.3 ± 24,898.6. In the ID + im1000 group it was 321,636.8 ± 23,133.7 and in the ID group the mean number of neurons was 330,868.3 ± 25,729.8. The CA1 area neuron count was practically the same across all three groups. The control group had a mean neuron count of 121,144.6 ± 31,641 the ID + im1000 group had one of 166,413.4 ± 17,928.3 and the ID group had 138,772.7 ± 12,719. The ID + im1000 group had a significantly larger amount of neurons in the DG area compared to the ID group ($p=0.038$). Otherwise, there were no significant differences between the other groups. See Table 4 and Figure 17.

	DG	CA2/3	CA1
Control	534.3 (±72.8)	180.5 (±24.9)	121.1 (±31.6)
ID + im1000	679.4 (±34.4)*	321.6 (±23.1)	166.4 (±17.9)
ID	494.1 (±26.9)	330.9 (±25.7)	138.8 (±12.7)

*Table 4: Mean number of neurons in the different areas of the hippocampus based on stereological counting of Control (n=2), ID + im1000 (n=8) and ID (n=3) animals. All values are x10³ ± SEM. *significantly larger than ID group (p<0,05)*

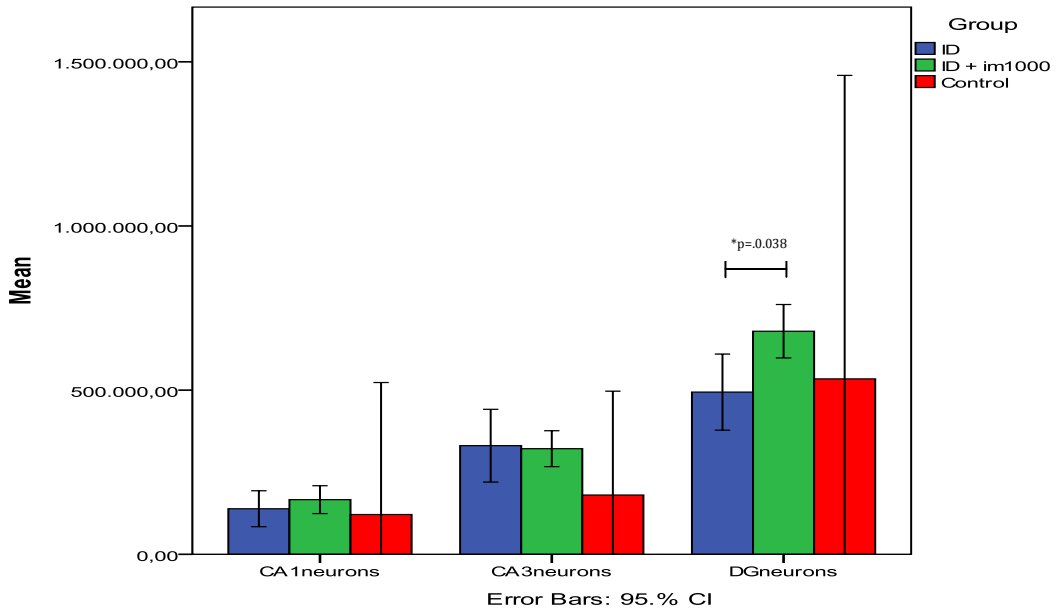

*Figure 17: The mean amount of neurons in the three areas of the hippocampus based on stereological counting of Control (n=2), ID + im1000 (n=8) and ID (n=3) animals. *Significant difference between the amount of neurons in the DG area of the ID + im1000 and the ID group (p=0.038)*

FREE FATTY ACID ANALYSIS

Several analyses were made of the fatty acid content in the phospholipid groups, PE, PS and PI, in the cerebellum. The total content of PUFAs was analyzed, and the percentage of fatty acids distributed over the n-3, n-6 and n-9 fatty acid groups were analyzed, along with the amount of DHA and C20:3n-3 which is also known as eicosatrienoic acid (ETE).

TOTAL PUFA CONTENT

The PUFA content in the phospholipidgroup PE was distributed as follows. The control group (N=7) had the highest mean PUFA content of 14.70% ± 1.99 while the ID + im1000 group (N=3) had the lowest mean of 6.24% ± 0.54. The ID group (N=5) had a mean PUFA content of 10.88% ± 1.22.
In the phospholipid group PS the control group (N=6) had the largest concentration of PUFAs with a mean of 10.18% ± 2.64 while the ID + im1000 group (N=6) had a mean of 4.28% ± 0.58 and the ID group (N=4) had 5.36% ± 1.63.
The mean content of PUFAs in the control group (N=7) of PI was 11.82% ± 1.99 whereas in the ID + im1000 group (N=6) it was 3.38% ± 0.60. In the ID group (N=5) the mean PUFA content was 7.93% ± 1.22.

In the PE and PI phospholipid groups there were significant differences between the total PUFA content of the control group and the ID + im1000 group (p=0.032 in PE and p=0.003 in PI) , while there was no difference between the groups in PS. (Figure 18)

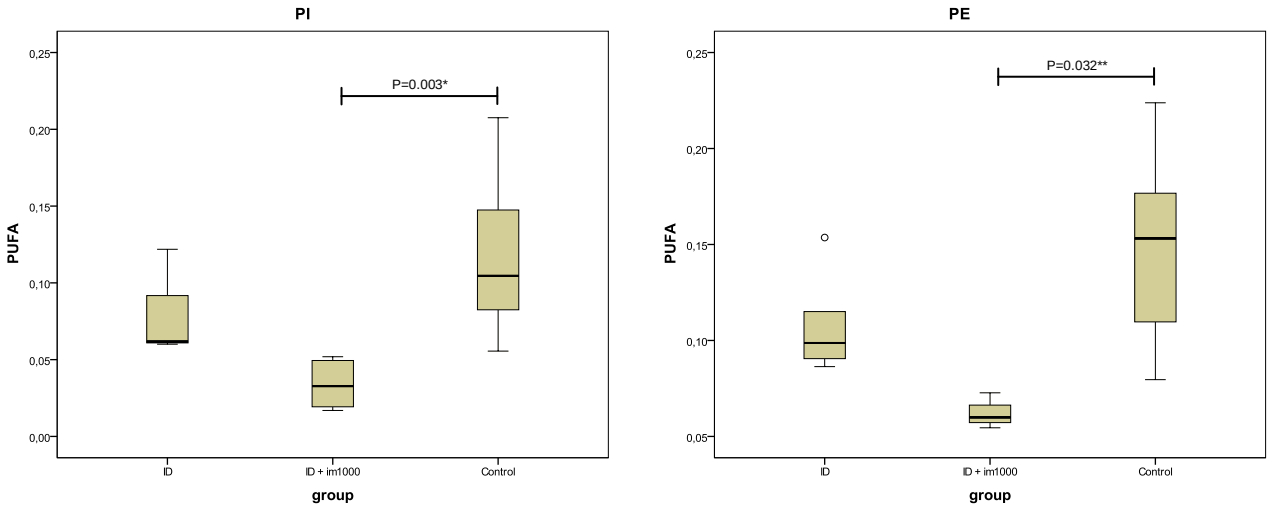

*Figure 18: Boxplot of the PUFA content in the phospholipid groups PE (left) and PI (right). *Significant difference between control and ID + im1000 groups in PI (p=0.003). **significant difference between control and ID + im1000 groups in PE (p=0.032)*

N-3, N-6 AND N-9 FATTY ACID DISTRIBUTION

In the phospholipid group PE, the control group had the largest amount of n-3 fatty acids at 12.31% ± 2.13 while the ID + im1000 group had 4.36% ± 0.48 and the ID group had a mean of 4.07% ± 0.38. The mean percentage of n-6 fatty acids were, however, lowest in the control group (0.11% ± 0.07) and the ID + im1000 group (0.18% ± 0.09) while the ID group had the highest values at 5.16% ± 0.58. The n-9 fatty acid amount was highest in the control group with a mean percentage of 2.28% ± 0.40. The ID + im1000 group had a mean value of 1.69% ± 0.20 while the ID group had 1.66% ± 0.32.
In PS the control group had the largest mean amount of n-3 fatty acids with a mean of 9.00% ± 2.78. The ID + im1000 group had a smaller mean amount of 3.08% ± 0.54 while the ID group had a mean of 3.33% ± 0.83. The control group had a mean amount of n-6 fatty acids of 0.28% ± 0.18 while the ID group had a mean of 1.76% ± 0.54. The ID + im1000 group had no n-6 fatty acids at all. The mean amount of n-9 fatty acids in the control group was 0.90% ± 0.41 and the ID + im1000 group had a mean of 1.20% ± 0.12 while the ID group had the smallest amount of 0.27% ± 0.27.
The control group had the largest mean amount of n-3 fatty acids in the phospholipid group PI with a mean of 10.43% ± 1.93 while the ID + im1000 group had a mean of 2.72% ± 0.45 and the ID had 2.23% ± 0.26. The control group had a mean n-6 fatty acid amount of 0.63% ± 0.49 and the ID + im1000 group had a mean of 0.38% ± 0.28 while the ID group had a larger mean of 4.43% ± 0.79. The largest mean amount of n-9 fatty acids belonged to the control group (0.76% ± 0.29) while the ID + im1000 group had a mean of 0.28% ± 0.18. The ID group contained 1.26% ± 0.22.

The amount of n-3 fatty acids were significantly larger in the control group than in the ID group (p=0.013) and the ID + im1000 group (p=0.043) in the PE phospholipid group, and the control group was significantly larger than the ID + im1000 group (p=0.002) and the ID group (p=0.002) in the PI phospholipid group.

Both the control and the ID + im1000 group contained significantly less n-6 fatty acids compared to the ID group in all the phospholipid groups ($p=0.001$ for both control-ID and ID + im1000-ID in PE; $p=0.002$ for control-ID and $p=0.001$ for ID + im1000-ID in PI; $p=0.015$ for control-ID and $p=0.047$ for ID + im1000-ID in PS).
There were no significant differences between groups in the amount of n-9 fatty acids. (Figure 19)

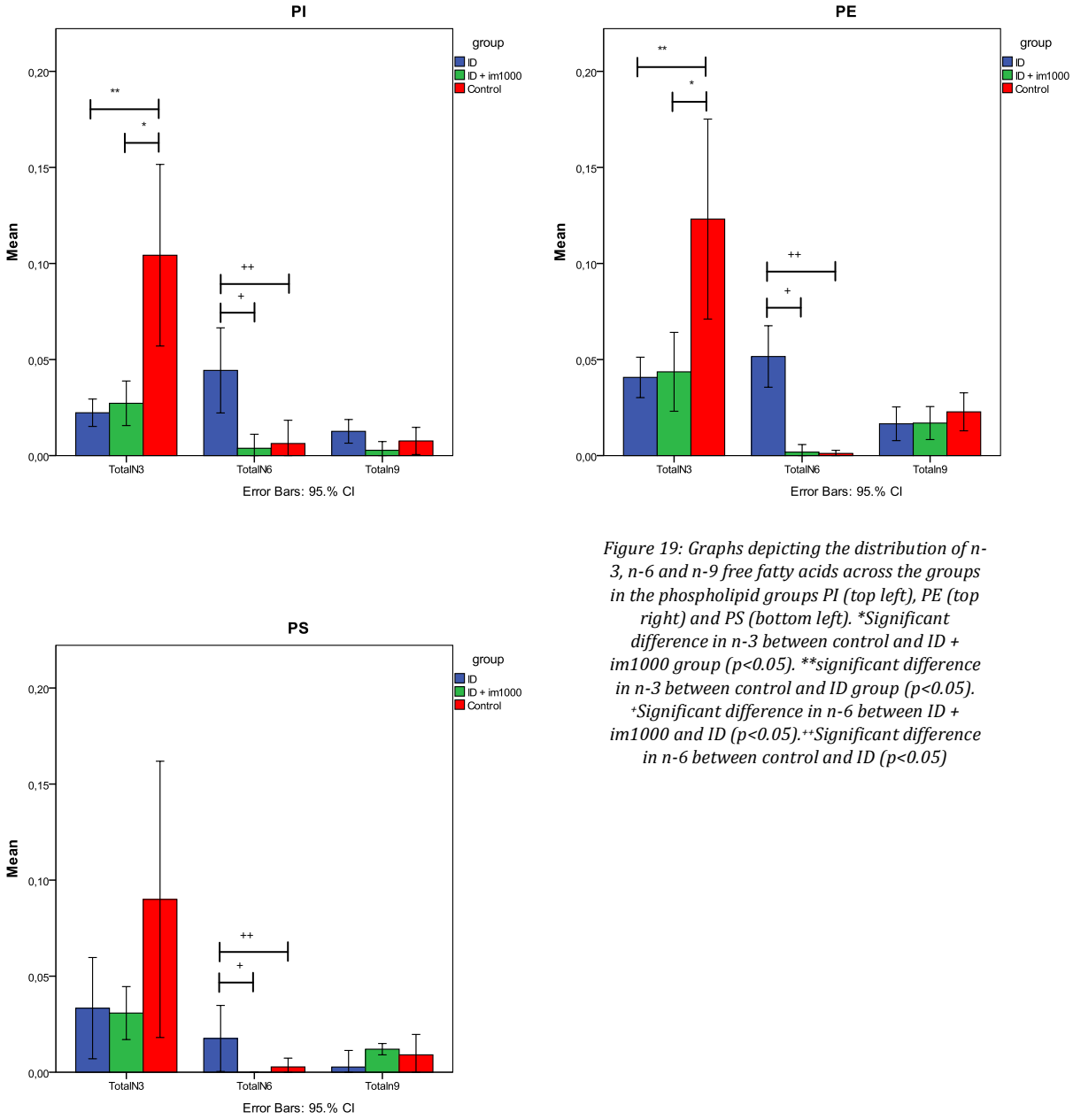

*Figure 19: Graphs depicting the distribution of n-3, n-6 and n-9 free fatty acids across the groups in the phospholipid groups PI (top left), PE (top right) and PS (bottom left). *Significant difference in n-3 between control and ID + im1000 group (p<0.05). **significant difference in n-3 between control and ID group (p<0.05). ⁺Significant difference in n-6 between ID + im1000 and ID (p<0.05).⁺⁺Significant difference in n-6 between control and ID (p<0.05)*

TOTAL AMOUNT OF DHA AND ETE

In the phospholipid group PE the largest amount of DHA was found in the control group with a mean percentage of 7.47% ± 1.36. The ID + im1000 group had a mean percentage of 1.84% ± 0.36 while the ID had a larger amount of 4.07% ± 0.38. The control group also had the largest amount of ETE as well with a mean percentage of 4.75% ± 0.83 and the ID + im1000 group had 2.53% ± 0.12 while the ID group had no ETE at all.

In PS the control group had the highest mean percentage of DHA with a mean of 6.73% ± 2.79 while the ID + im1000 group had the lowest of 1.15% ± 0.29. The ID group had a mean DHA percentage of 3.33% ± 0.83. The control group and the ID + im1000 group had approximately the same mean percentage of ETE, the control group having a mean of 2.26% ± 0.63 and the ID + im1000 one of 1.93% ± 0.30. The ID group did not contain any ETE.
In PI the control group had the largest amount of DHA with a mean of 4.71% ± 1.40 while the ID + im1000 group had a somewhat smaller mean of 0.43% ± 0.27. The ID group had a mean DHA percentage of 2.23% ± 0.26. The greatest amount of ETE was also found in the control group (5.59% ± 1.17), while the ID + im1000 group contained a smaller amount namely 2.30% ± 0.27 and the ID group did not contain any ETE.

In the phospholipid group PE the control group had a significantly larger amount of DHA than the ID + im1000 group (p=0.026) and in the PI the ID + im1000 group contained a smaller amount of DHA than both the control group (p=0.018) and the ID group (p=0.001). There was no difference in DHA content across the groups in PS. (Figure 20)
In the PE phospholipid group there was a significantly larger amount of ETE in the control group compared to the ID group (p=0.001). In PI the control group had a significantly larger content of ETE than both the ID group (p=0.001) and the ID + im1000 group (p=0.029). In PS the ID group had a significantly smaller content of ETE than the control group (p=0.017) and the ID + im1000 group (p=0.043), see Figure 21.
All results from the fatty acid analyses can be seen in Table 5.

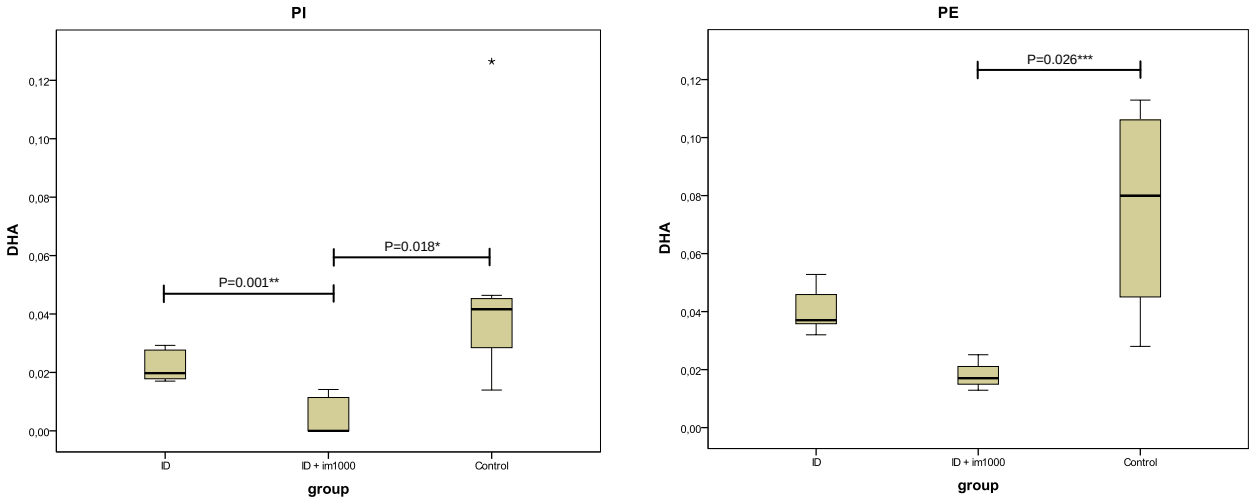

*Figure 20: Boxplot of the DHA content of the groups in PI (left) and PE (right).*Significant difference between control and ID + im1000 groups in PI (p=0.018). **Significant difference between ID and ID + im1000 groups in PI (p=0.001). ***Significant difference between control and ID + im1000 groups in PE (p=0.026)*

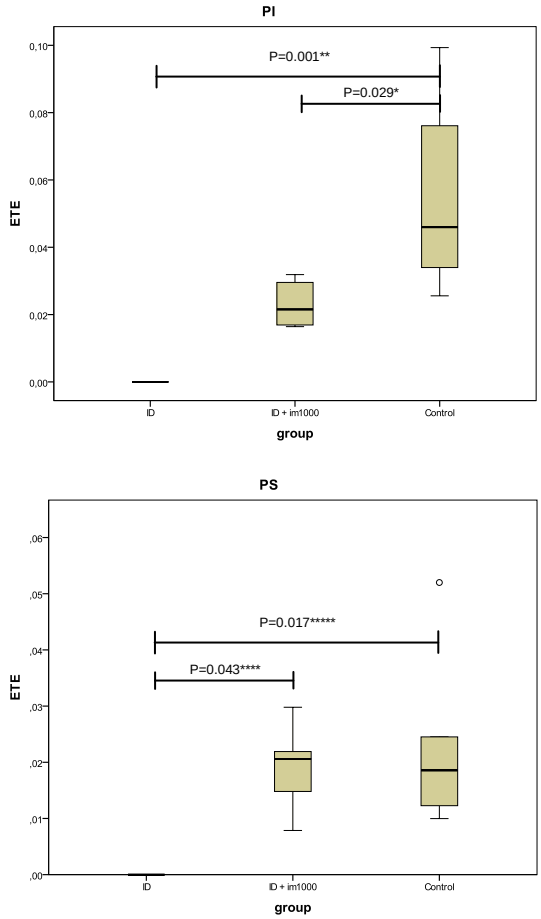

*Figure 21: Boxplot depicting the distribution of ETE among the groups in PI (top left), PE (top right) and PS (bottom left). *Significant difference between control and ID + im1000 group in PI (p=0.029). **Significant difference between control and ID groups in PI (p=0.001). ***Significant difference between control and ID groups in PE (p=0.001). ****Significant difference between ID + im1000 and ID groups in PS (p=0.043). *****Significant difference between control and ID groups in PS (p=0.017)*

PE

Group	DHA	ETE	Total PUFA	Total n-3	Total n-6	Total n-9
Control	7.47[5] (±1.36)	4.75[2] (±0.83)	14.70[5] (±1.99)	12.31[1,5] (±2.13)	0.11[2] (±0.07)	2.28 (±0.40)
ID + im1000	1.84[3] (±0.36)	2.53 (±0.12)	6.24[3] (±0.54)	4.36[3] (±0.48)	0.18[2] (±0.09)	1.69 (±0.20)
ID	4.07 (±0.38)	0[4] (±0)	10.88 (±1.22)	4.07[3] (±0.38)	5.16[4,6] (±0.58)	1.66 (±0.32)
PI						
Control	4.71[5] (±1.40)	5.59[2,5] (±1.17)	11.82[5] (±1.99)	10.43[1,5] (±1.93)	0.63[1] (±0.49)	0.76 (±0.29)
ID + im1000	0.43[2,3] (±0.27)	2.30[3] (±0.27)	3.38[3] (±0.60)	2.72[3] (±0.45)	0.38[2] (±0.28)	0.28 (±0.18)
ID	2.23[6] (±0.26)	0[4] (±0)	7.93 (±1.22)	2.23[3] (0.26)	4.43[3,6] (±0.79)	1.26 (±0.22)
PS						
Control	6.73 (±2.79)	2.26[1] (±0.63)	10.18 (±2.64)	9.00 (±2.78)	0.28[1] (±0.18)	0.90 (±0.41)
ID + im1000	1.15 (±0.29)	1.93[1] (±0.30)	4.28 (±0.58)	3.08 (±0.54)	0[1] (±0)	1.20 (±0.12)
ID	3.33 (±0.83)	0[3,5] (±0)	5.36 (±1.63)	3.33 (±0.83)	1.76[3,5] (±0.54)	0.27 (±0.27)

Table 5: All values are stated as % ± SEM. [1]: significantly different from ID ($p<0.05$) [2]: significantly different from ID ($p<0.01$) [3]: significantly different from Control ($p<0.05$) [4]: significantly different from Control ($p<0.01$) [5]: significantly different from ID + im1000 ($p<0.05$) [6]: significantly different from ID + im1000 ($p<0.01$)

DISCUSSION

One of the most evident signs of iron deficiency is altered hematological data manifested by decreased hct and hemoglobin values. In this study hct values were obtained to verify the presence of iron deficiency and to monitor the severity at different time points of the study. Blood tests confirmed that exsanguination of dams followed by an iron restricted diet was an effective way of ensuring offspring with severe iron deficiency anemia. Further, results showed that the hct level in ID rats was significantly lower at all times compared to both control and ID + im1000 animals. However, the severity of iron deficiency changed over time, with low hct values obtained in the weaning period (P8-P13 and P15-P18) and an increased level as the rats reached adulthood (P86-P94). This indicates that iron deficiency is more pronounced during the growth spurt, possibly due to a substantial need of iron in this period of rapid growth. When considering the last hct measurement it is important to note that some of the most undernourished and weak ID rats died during the study period. Thus the observed increase in hct measurement in the ID rats might be related to the survival of the better nourished rats.
When obtaining blood tests for hct determination, an interesting observation was made. The blood plasma from the ID rats appeared opaque and white compared to the transparent plasma obtained from the control and ID + im1000 rats. This suggests an accumulation of fatty acids in the blood plasma due to an altered fatty acid metabolism or transport. The function of essential iron-dependant liver enzymes may be compromised due to a severe lack of iron, which leads to alterations of lipoprotein or albumin biogenesis. The accumulation of fatty acids in blood plasma may be related to a compromised beta oxidation of fatty acids. A study using intestinal RNA from rats demonstrated a connection between iron deficiency and dyslipidemia. Microarray analysis revealed a 20 fold decrease in RNA expression of the apolipoprotein H and down regulation of several genes involved with beta oxidation. Although the exact function of this protein is not completely characterized, it is suggested to maintain triglyceride clean-up from plasma. Moreover, apolipoprotein H influences the balance of cholesterol influx and efflux. ([74]) Thus, iron deficiency mediated down regulation of genes involved with fatty acid metabolism may represent a plausible explanation for the change in blood plasma appearance.
The results from the footprint analysis showed that ID rats had a significantly larger gait width compared to both ID + im1000 and control rats. However, no significant difference was observed in stride length between the groups. These results indicate that iron deficient rats have poorer motor coordination and balance skills compared to ID + im1000 and control rats, possibly caused by alterations in the nigrostriatal pathway ([75]) and cerebellar processes. A study by Yu et al ([76]) showed that rats with prenatal iron deficiency had less myelinated areas of the brain, there amongst the cerebellum, than rats of a similar age that were not ID. The impaired function of the cerebellum arising from impaired myelination along with alterations in the nigrostrital pathway would explain the poor results exhibited by the ID rats.
Analysis of total iron content from the mesencephalon revealed a significant difference between iron deficient rats and controls, which is in accordance with previous studies ([42,46]). Furthermore, iron supplementation improved the total concentration of iron in the mesencephalon and a significant difference could be detected between ID + im1000 and ID rats. No significant difference was found between ID + im1000 and control rats which suggests that perinatal iron deficiency can be completely reverted with early administration of iron supplementation.

Stereological counting of the neurons in the hippocampus of the animals revealed a significant difference in the amount of neurons in the DG between ID + im1000 rats and ID rats. To my knowledge, no stereological studies of the hippocampus of ID animals have been published yet. The expression of cytochrome c oxidase, which is a marker of neuronal metabolic activity, has been observed to decrease in all hippocampal areas as a result of gestational ID, which suggests that a reduction in the neuron count of all hippocampal areas would be observed ([77]). Unfortunately this study cannot argue for or against these observations, as the control group does not contain enough animals to determine whether ID does reduce the amount of neurons compared to normal animals. It does, however, show that iron supplementation increases the amount of neurons in the DG. Studies have shown that approximately 9000 new neurons are generated in the hippocampus of healthy young adult rats each day ([78]). However, stressful experiences as well as old age have been shown to decrease the amount of neurons that are generated ([79]) leading to the assumption that severe iron deficiency inhibits neurogenesis through a combination of stress and impaired DNA synthesis. The results suggest that injected iron isomaltoside 1000 during early life in rats, which roughly correlates to the third trimester of human development ([80]), can increase the amount of neurons in the hippocampus and quite possibly the function as well. Other studies suggest that the effects of congenital ID on the hippocampus persist even after normal iron levels have been established ([81]), which may well be the case, as the low amount of tissue which was successfully counted stereologically makes it difficult to draw definite conclusions.

The FFA analysis revealed that the total PUFA content of the cerebellum in the control animals is consequently, albeit not significantly, higher than that of the ID animals. It is, however, significantly higher than that of the ID + im1000 animals in two out of the three phospholipid groups which were analyzed. A study conducted on mice showed significantly smaller PUFA content in the brain lipid composition of mice with gestational ID compared to control mice which is in accordance with this study, but it also showed that mice which were put back on a iron-replete diet containing 75µg Fe/g had similar levels of PUFA as the control mice, which is in direct contrast to this study ([82]). The difference in the results might be due to the severity of the iron deficiency that the animals used in this study suffered from, or from the method of repleting the ID animals. The results suggest that iron deficiency does alter the PUFA content of the brain, and that iron supplementation may recover the PUFA content, depending on the severity of iron deficiency. The results also suggest that highly bioavailable iron supplementation might have a deleterious effect on the PUFA content in the brain, possibly by acting as free radicals since PUFAs easily suffer oxidation ([83]).

The levels of n-3 FFAs were significantly higher in the control animals compared to both the ID and ID + im1000 animals in two of the three phospholipid groups. The levels of n-6 FFAs were significantly lower in both the control and the ID + im1000, when compared to the ID rats which had between 6 and 28 times higher amounts of n-6 FFAs depending on the phospholipid group. The results imply that congenital iron deficiency reduces the amount of n-3 FAs and increases the amount of n-6 FAs in the cerebellum of rats, and that the n-3 deficit cannot be recovered using iron supplementation in the neonatal rats. The ratio of n-6:n-3 FAs effects the ratio of their ensuing eicosanoids (e.g. prostaglandins and leukotrienes) of which the n-6 eicosanoids are generally pro-inflammatory, while the n-3 eicosanoids are much less so ([84]). The results suggest that eventual deleterious effects of an increased n-6:n-3 ratio caused by congenital iron deficiency can be avoided by use of iron supplementation.
The amount of DHA in the cerebellum seemed to decline in the animals receiving iron isomaltoside 1000 supplementation, while the levels of ETE were somewhat recovered in the ID + im1000 rats. This

leads to the assumption that the formation of ETE relies heavily on iron-dependant enzymes, since it was not present in the ID rats, and that while the DHA levels seemingly drop as a result of iron supplementation, the ETE levels are recovered to some extent.

The importance of iron during development cannot be understated. To avoid the deleterious effects of iron deficiency, treatment is necessary. Iron can be administered in different forms with dietary supplement being the far most prevalent absorption mechanism of the body ([85]). Intravenous iron injections are another possibility with the clear advantage of a higher bioavailability. Iron injections are applied when oral iron is poorly tolerated and rapid replacement of iron stores is needed, especially during severe iron deficiency ([85]). When applying iron supplements to treat congenital iron deficiency, the timing is a crucial factor to be considered. A study by Beard et al. suggested that a window of opportunity for iron treatment exists ([86]). The results of the study proposed that perinatal iron deficiency in rats should be treated during early lactation, which roughly correlates with the start of the 3rd trimester in terms of human development, in order to attain full remission ([86, 80]).
In this study iron administration began at P4 in order to ensure early iron repletion. Results showed evidence that the deleterious effects of congenital ID can be reversed to some degree by administering iron isomaltoside 1000 during the 3rd trimester of pregnancy. While motor defects and low hematological values resulting from congenital ID are reversed completely, the results suggest that the lipid composition of the cerebellum cannot be fully recovered to that of normal individuals.
Furthermore, the results suggest that an increase in neurogenisis occur in the DG of rats receiving iron supplement, possibly by relieving the animals of stress associated with iron deficiency while adding the iron that is needed for optimal DNA synthesis.
This illustrates the complexity of treating iron deficiency correctly in order to attain full recovery. In addition, it is important to take into account, that iron excess is as detrimental as iron deficiency, for which reason the exact dose of highly bioavailable iron must be explored more extensively to avoid overload in patients who are treated with iron injections.

REFERENCES

1. Bohnsack BL, Hirschi KK. Nutrient regulation of cell cycle progression. Annu Rev Nutr. 2004;24:433-53.
2. Todorich B, Pasquini JM, Garcia CI, Paez PM, Connor JR. Oligodendrocytes and myelination: the role of iron. Glia. 2009 Apr 1;57(5):467-78.
3. Crichton R. Iron metabolism - From molecular mechanisms to clinical consequences. 3rd ed.: John Wiley & Sons Ltd; 2009.
4. Stoltzfus RJ. Iron-deficiency anemia: reexamining the nature and magnitude of the public health problem. Summary: implications for research and programs. J Nutr. 2001 Feb;131(2S-2):697S-700S; discussion S-1S.
5. Lozoff B. Iron deficiency and child development. Food Nutr Bull. 2007 Dec;28(4 Suppl):S560-71.
6. Gambling L, Andersen HS, McArdle HJ. Iron and copper, and their interactions during development. Biochem Soc Trans. 2008 Dec;36(Pt 6):1258-61.
7. Rodgers A, Vaughan P. The world health report 2002, reducing risks, promoting healthy life; 2002 Contract No.: Document Number|.
8. Georgieff MK. The role of iron in neurodevelopment: fetal iron deficiency and the developing hippocampus. Biochem Soc Trans. 2008 Dec;36(Pt 6):1267-71.
9. Dallman PR. Biochemical basis for the manifestations of iron deficiency. Annu Rev Nutr. 1986;6:13-40.
10. Baynes J, Dominiczak mh. Medical Biochemistry. 1 ed.: Mosby; 1999.
11. Sharp P, Srai SK. Molecular mechanisms involved in intestinal iron absorption. World J Gastroenterol. 2007 Sep 21;13(35):4716-24.
12. McKie AT, Barrow D, Latunde-Dada GO, Rolfs A, Sager G, Mudaly E, et al. An iron-regulated ferric reductase associated with the absorption of dietary iron. Science. 2001 Mar 2;291(5509):1755-9.
13. Dorey C, Cooper C, Dickson DP, Gibson JF, Simpson RJ, Peters TJ. Iron speciation at physiological pH in media containing ascorbate and oxygen. Br J Nutr. 1993 Jul;70(1):157-69.
14. Han O, Failla ML, Hill AD, Morris ER, Smith JC, Jr. Reduction of Fe(III) is required for uptake of nonheme iron by Caco-2 cells. J Nutr. 1995 May;125(5):1291-9.
15. Glahn RP, Van Campen DR. Iron uptake is enhanced in Caco-2 cell monolayers by cysteine and reduced cysteinyl glycine. J Nutr. 1997 Apr;127(4):642-7.
16. Swain JH, Tabatabai LB, Reddy MB. Histidine content of low-molecular-weight beef proteins influences nonheme iron bioavailability in Caco-2 cells. J Nutr. 2002 Feb;132(2):245-51.
17. Gunshin H, Mackenzie B, Berger UV, Gunshin Y, Romero MF, Boron WF, et al. Cloning and characterization of a mammalian proton-coupled metal-ion transporter. Nature. 1997 Jul 31;388(6641):482-8.
18. Hubert N, Hentze MW. Previously uncharacterized isoforms of divalent metal transporter (DMT)-1: implications for regulation and cellular function. Proc Natl Acad Sci U S A. 2002 Sep 17;99(19):12345-50.
19. Tandy S, Williams M, Leggett A, Lopez-Jimenez M, Dedes M, Ramesh B, et al. Nramp2 expression is associated with pH-dependent iron uptake across the apical membrane of human intestinal Caco-2 cells. J Biol Chem. 2000 Jan 14;275(2):1023-9.
20. Hallberg L. Bioavailability of dietary iron in man. Annu Rev Nutr. 1981;1:123-47.
21. Shayeghi M, Latunde-Dada GO, Oakhill JS, Laftah AH, Takeuchi K, Halliday N, et al. Identification of an intestinal heme transporter. Cell. 2005 Sep 9;122(5):789-801.
22. Parmley RT, Barton JC, Conrad ME, Austin RL, Holland RM. Ultrastructural cytochemistry and radioautography of hemoglobin--iron absorption. Exp Mol Pathol. 1981 Apr;34(2):131-44.

23. Arosio P, Levi S. Ferritin, iron homeostasis, and oxidative damage. Free Radic Biol Med. 2002 Aug 15;33(4):457-63.
24. Hunt JR, Roughead ZK. Nonheme-iron absorption, fecal ferritin excretion, and blood indexes of iron status in women consuming controlled lactoovovegetarian diets for 8 wk. Am J Clin Nutr. 1999 May;69(5):944-52.
25. Anderson GJ, Frazer DM, McLaren GD. Iron absorption and metabolism. Curr Opin Gastroenterol. 2009 Mar;25(2):129-35.
26. Donovan A, Brownlie A, Zhou Y, Shepard J, Pratt SJ, Moynihan J, et al. Positional cloning of zebrafish ferroportin1 identifies a conserved vertebrate iron exporter. Nature. 2000 Feb 17;403(6771):776-81.
27. Park CH, Valore EV, Waring AJ, Ganz T. Hepcidin, a urinary antimicrobial peptide synthesized in the liver. J Biol Chem. 2001 Mar 16;276(11):7806-10.
28. Vulpe CD, Kuo YM, Murphy TL, Cowley L, Askwith C, Libina N, et al. Hephaestin, a ceruloplasmin homologue implicated in intestinal iron transport, is defective in the sla mouse. Nat Genet. 1999 Feb;21(2):195-9.
29. Chen H, Attieh ZK, Su T, Syed BA, Gao H, Alaeddine RM, et al. Hephaestin is a ferroxidase that maintains partial activity in sex-linked anemia mice. Blood. 2004 May 15;103(10):3933-9.
30. Cheng Y, Zak O, Aisen P, Harrison SC, Walz T. Structure of the human transferrin receptor-transferrin complex. Cell. 2004 Feb 20;116(4):565-76.
31. Moos T, Rosengren Nielsen T, Skjorringe T, Morgan EH. Iron trafficking inside the brain. J Neurochem. 2007 Dec;103(5):1730-40.
32. Angelova-Gateva P. Iron transferrin receptors in rat and human cerebrum. Agressologie. 1980;21(1):27-30.
33. Benarroch EE. Brain iron homeostasis and neurodegenerative disease. Neurology. 2009 Apr 21;72(16):1436-40.
34. Burdo JR, Menzies SL, Simpson IA, Garrick LM, Garrick MD, Dolan KG, et al. Distribution of divalent metal transporter 1 and metal transport protein 1 in the normal and Belgrade rat. J Neurosci Res. 2001 Dec 15;66(6):1198-207.
35. Ke Y, Chang YZ, Duan XL, Du JR, Zhu L, Wang K, et al. Age-dependent and iron-independent expression of two mRNA isoforms of divalent metal transporter 1 in rat brain. Neurobiol Aging. 2005 May;26(5):739-48.
36. Moos T, Rosengren Nielsen T. Ferroportin in the postnatal rat brain: implications for axonal transport and neuronal export of iron. Semin Pediatr Neurol. 2006 Sep;13(3):149-57.
37. Moos T, Morgan EH. Kinetics and distribution of [59Fe-125I]transferrin injected into the ventricular system of the rat. Brain Res. 1998 Apr 20;790(1-2):115-28.
38. Schroeder T. Basisbog i medicin og kirurgi. Kbh.: Munksgaard Danmark; 2004.
39. LeBlanc CP, Fiset S, Surette ME, Turgeon O'Brien H, Rioux FM. Maternal iron deficiency alters essential fatty acid and eicosanoid metabolism and increases locomotion in adult guinea pig offspring. J Nutr. 2009 Sep;139(9):1653-9.
40. Morath DJ, Mayer-Proschel M. Iron modulates the differentiation of a distinct population of glial precursor cells into oligodendrocytes. Dev Biol. 2001 Sep 1;237(1):232-43.
41. Connor JR, Menzies SL. Relationship of iron to oligodendrocytes and myelination. Glia. 1996 Jun;17(2):83-93.
42. Beard JL, Wiesinger JA, Connor JR. Pre- and postweaning iron deficiency alters myelination in Sprague-Dawley rats. Dev Neurosci. 2003 Sep-Oct;25(5):308-15.
43. Jin Y. Synaptogenesis. WormBook. 2005:1-11.
44. Vicario-Abejon C, Collin C, McKay RD, Segal M. Neurotrophins induce formation of functional excitatory and inhibitory synapses between cultured hippocampal neurons. J Neurosci. 1998 Sep 15;18(18):7256-71.
45. Tran PV, Carlson ES, Fretham SJ, Georgieff MK. Early-life iron deficiency anemia alters neurotrophic factor expression and hippocampal neuron differentiation in male rats. J Nutr. 2008 Dec;138(12):2495-501.

46. Jorgenson LA, Wobken JD, Georgieff MK. Perinatal iron deficiency alters apical dendritic growth in hippocampal CA1 pyramidal neurons. Dev Neurosci. 2003 Nov-Dec;25(6):412-20.
47. Goodman LS, Gilman A, Brunton LL, Parker KL. Goodman & Gilman's manual of pharmacology and therapeutics. New York: McGraw-Hill Medical; 2008.
48. Lozoff B, Georgieff MK. Iron deficiency and brain development. Semin Pediatr Neurol. 2006 Sep;13(3):158-65.
49. Youdim MB. Brain iron deficiency and excess; cognitive impairment and neurodegeneration with involvement of striatum and hippocampus. Neurotox Res. 2008 Aug;14(1):45-56.
50. Bianco LE, Wiesinger J, Earley CJ, Jones BC, Beard JL. Iron deficiency alters dopamine uptake and response to L-DOPA injection in Sprague-Dawley rats. J Neurochem. 2008 Jul;106(1):205-15. Epub 2008 Jul 1.
51. Beard J, Erikson KM, Jones BC. Neonatal iron deficiency results in irreversible changes in dopamine function in rats. J Nutr. 2003 Apr;133(4):1174-9.
52. Erikson KM, Jones BC, Beard JL. Iron deficiency alters dopamine transporter functioning in rat striatum. J Nutr. 2000 Nov;130(11):2831-7.
53. Beard JL, Connor JR. Iron status and neural functioning. Annu Rev Nutr. 2003;23:41-58.
54. Lozoff B, Klein NK, Nelson EC, McClish DK, Manuel M, Chacon ME. Behavior of infants with iron-deficiency anemia. Child Dev. 1998 Feb;69(1):24-36.
55. Lukowski AF, Koss M, Burden MJ, Jonides J, Nelson CA, Kaciroti N, Jimenez E, Lozoff B. Iron deficiency in infancy and neurocognitive functioning at 19 years: evidence of long-term deficits in executive function and recognition memory. Nutr Neurosci. 2010 Apr;13(2):54-70.
56. Schuchardt JP, Huss M, Stauss-Grabo M, Hahn A. Significance of long-chain polyunsaturated fatty acids (PUFAs) for the development and behaviour of children. Eur J Pediatr. 2010 Feb;169(2):149-64.
57. Van Gelder BM, Tijhuis M, Kalmijn S, Kromhout D. Fish consumption, n-3 fatty acids, and subsequent 5-y cognitive decline in elderly men: the Zutphen Elderly Study.Am J Clin Nutr. 2007 Apr;85(4):1142-7.
58. Issa AM, Mojica WA, Morton SC, Traina S, Newberry SJ, Hilton LG, Garland RH, Maclean CH. The efficacy of omega-3 fatty acids on cognitive function in aging and dementia: a systematic review. Dement Geriatr Cogn Disord. 2006;21(2):88-96.
59. Lukiw WJ, Bazan NG. Survival signalling in Alzheimer's disease. Biochem Soc Trans. 2006 Dec;34(Pt 6):1277-82.
60. Neuringer M, Anderson GJ, Connor WE. The essentiality of n-3 fatty acids for the development and function of the retina and brain. Annu Rev Nutr. 1988;8:517-41.
61. Jeffrey BG, Weisinger HS, Neuringer M, Mitchell DC. The role of docosahexaenoic acid in retinal function. Lipids. 2001 Sep;36(9):859-71.
62. Uauy R, Dangour AD. Nutrition in brain development and aging: role of essential fatty acids. Nutr Rev. 2006 May;64(5 Pt 2):S24-33; discussion S72-91.
63. Transler C, Eilander A, Mitchell S, van de Meer N. The impact of polyunsaturated fatty acids in reducing child attention deficit and hyperactivity disorders. J Atten Disord. 2010 Nov;14(3):232-46.
64. Burdge GC, Calder PC. Conversion of alpha-linolenic acid to longer-chain polyunsaturated fatty acids in human adults. Reprod Nutr Dev. 2005 Sep-Oct;45(5):581-97.
65. Pawlosky RJ, Hibbeln JR, Novotny JA, Salem N Jr. Physiological compartmental analysis of alpha-linolenic acid metabolism in adult humans. J Lipid Res. 2001 Aug;42(8):1257-65.
66. West MJ, Slomianka L, Gundersen HJ. Unbiased stereological estimation of the total number of neurons in thesubdivisions of the rat hippocampus using the optical fractionator.Anat Rec. 1991 Dec;231(4):482-97.
67. Lorente de Nó R. Studies on the structure of the cerebral cortex. II Continuation of the study of the ammonic system. J.Psychol.Neurol. 1934;46:113-177.

68. Martin SJ, Clark RE. The rodent hippocampus and spatial memory: from synapses to systems. Cell Mol Life Sci. 2007 Feb;64(4):401-31.
69. Drapeau E, Mayo W, Aurousseau C, Le Moal M, Piazza PV, Abrous DN. Spatial memory performances of aged rats in the water maze predict levels of hippocampal neurogenesis. Proc Natl Acad Sci U S A. 2003 Nov 25;100(24):14385-90.
70. Montaron MF, Drapeau E, Dupret D, Kitchener P, Aurousseau C, Le Moal M, Piazza PV, Abrous DN. Lifelong corticosterone level determines age-related decline in neurogenesis and memory. Neurobiol Aging. 2006 Apr;27(4):645-54.
71. Campbell S, Macqueen G. The role of the hippocampus in the pathophysiology of major depression. J Psychiatry Neurosci. 2004 Nov;29(6):417-26.
72. De Kloet ER, Vreugdenhil E, Oitzl MS, Joëls M. Brain corticosteroid receptor balance in health and disease. Endocr Rev. 1998 Jun;19(3):269-301.
73. Ulrich-Lai YM, Herman JP. Neural regulation of endocrine and autonomic stress responses. Nat Rev Neurosci. 2009 Jun;10(6):397-409.
74. Tosco A, Fontanella B, Danise R, Cicatiello L, Grober OM, Ravo M, et al. Molecular bases of copper and iron deficiency-associated dyslipidemia: a microarray analysis of the rat intestinal transcriptome. Genes Nutr. 2009 Oct 11.
75. Klein A, Wessolleck J, Papazoglou A, Metz GA, Nikkhah G. Walking pattern analysis after unilateral 6-OHDA lesion and transplantation of foetal dopaminergic progenitor cells in rats. Behav Brain Res. 2009 May 16;199(2):317-25.
76. Yu GS, Steinkirchner TM, Rao GA, Larkin EC. Effect of prenatal iron deficiency on myelination in rat pups. Am J Pathol. 1986 Dec;125(3):620-4.
77. de Deungria M, Rao R, Wobken JD, Luciana M, Nelson CA, Georgieff MK. Perinatal iron deficiency decreases cytochrome c oxidase (CytOx) activity in selected regions of neonatal rat brain. Pediatr Res. 2000 Aug;48(2):169-76.
78. Cameron HA, McKay RD. Adult neurogenesis produces a large pool of new granule cells in the dentate gyrus. J Comp Neurol. 2001 Jul 9;435(4):406-17.
79. Shors TJ, Anderson ML, Curlik DM 2nd, Nokia MS. Use it or lose it: How neurogenesis keeps the brain fit for learning. Behav Brain Res. 2011 Apr 22.
80. Clancy B, Darlington RB, Finlay BL. Translating developmental time across mammalian species. Neuroscience. 2001;105(1):7-17.
81. Tran PV, Fretham SJ, Carlson ES, Georgieff MK. Long-term reduction of hippocampal brain-derived neurotrophic factor activity after fetal-neonatal iron deficiency in adult rats. Pediatr Res. 2009 May;65(5):493-8.
82. Kwik-Uribe CL, Gietzen D, German JB, Golub MS, Keen CL. Chronic marginal iron intakes during early development in mice result in persistent changes in dopamine metabolism and myelin composition. J Nutr. 2000 Nov;130(11):2821-30.
83. Spiteller G. Peroxyl radicals: inductors of neurodegenerative and other inflammatory diseases. Their origin and how they transform cholesterol, phospholipids, plasmalogens, polyunsaturated fatty acids, sugars, and proteins into deleterious products. Free Radic Biol Med. 2006 Aug 1;41(3):362-87.
84. Fritsche K. Fatty acids as modulators of the immune response. Annu Rev Nutr. 2006;26:45-73.
85. Schroeder TV, Schulze S, Hilsted J, Aldershvile J, editors. Basisbog i Medicin og Kirurgi. 3. ed. København: Munksgaard Danmark; 2005.
86. Beard JL, Unger EL, Bianco LE, Paul T, Rundle SE, Jones BC. Early postnatal iron repletion overcomes lasting effects of gestational iron deficiency in rats. J Nutr. 2007 May;137(5):1176-82.